 doi:10.20944/preprints202209.0320.v1

Review

The Tetrahydrofuran Motif in Marine Lipids and Terpenes

Paula González-Andrés[1], Laura Fernández-Peña[1], Carlos Díez-Poza[2,*] and Asunción Barbero[1,*]

1 Department of Organic Chemistry, Campus Miguel Delibes, University of Valladolid, 47011 Valladolid, Spain; laura.fernandez.pena@uva.es (L.F.-P.); carlos.diez@uva.es (C.D.-P.); paula.gonzalez.andres@uva.es (P.G.-A.)
2 Department of Inorganic Chemistry, Faculty of Pharmacy, University of Alcalá de Henares, 28871 Alcalá de Henares, Spain.
* Correspondence: asuncion.barbero@uva.es, carlos.diezp@uah.es

Abstract: heterocycles are particularly common moieties within marine natural products. Specifically, tetrahydrofuranyl rings are present in a variety of compounds which present complex structures and interesting biological activities. Focusing on terpenoids, a high number of tetrahydrofuran-containing metabolites have been isolated during the last decades. They show promising biological activities, making them potential leads for novel antibiotics, antikinetoplastid drugs, amoebicidal substances or anticancer drugs. Thus, they have attracted the attention of the synthetic community, and numerous approaches to their total syntheses have appeared. Here, we offer the reader an overview of marine-derived terpenoids and related compounds, with a special focus on their isolation, structure determination, biological profiles and total syntheses.

Keywords: marine natural products; oxygen heterocycles; tetrahydrofuran; total synthesis; biological activity; terpenes; fatty acids.

1. Introduction

Marine organisms are a source of intriguing and fascinating compounds. These living beings have continuously evolved over time, since they are part of the oldest habitat on earth. Being also the largest ecosystem, it has the potential to offer innumerable compounds with interesting biological activities yet to be discovered. This is supported by the fact that hundreds of new molecules are reported within the scientific community every year.

Usually, the isolation of pure active compounds is a time-consuming and expensive process, due to the need of efficient extraction processes and sequential purification steps. Moreover, large amounts of raw materials have to be collected to finally isolate fairly low quantities of the desired compounds.

Fortunately, the great contribution of chemists in the field of total synthesis and asymmetric catalysis over the last decades has had countless benefits. On one hand, even though nuclear magnetic resonance (NMR) techniques are very powerful tools, in some cases the characterization of complex molecules can be difficult, leading to misassignments [1]. Fortunately, total synthesis has emerged as a – somewhat - costly but effective tool for the determination of the absolute configuration of marine metabolites. On the other hand, synthesis provides access to sufficient quantities of the desired compounds for further extensive biological studies.

Within the marine-derived metabolites, terpenes represent one of the most significant families. They are a large and diverse group of compounds that usually present valuable pharmacological properties. Marine-derived fungi are an important source of terpenes and various reviews summarize the discovery of high number of these metabolites in recent years [2-4].

Preprints (www.preprints.org) | NOT PEER-REVIEWED | Posted: 21 September 2022 doi:10.20944/preprints202209.0320.v1

Other common structural motifs present in marine drugs are heterocycles. Within them, five-, six-, and seven-membered oxygenated heterocycles, are frequently found in such bioactive compounds. The six-membered tetrahydropyrans, the most abundant, are common targets of study [5, 6]. The corresponding seven-membered oxepanes, and their appearance in relevant bioactive marine compounds, were reviewed by our group [7]. Regarding tetrahydrofurans, Fernandes and coworkers lately reviewed the most iconic examples of total synthesis of 2,3,5-trisubstituted tetrahydrofuran-containing natural products [8], [9]. We have also recently summarized the synthesis and biological properties of marine-derived tetrahydrofuran-containing compounds, focusing on the polyketide family[10].

Continuing our series, here we give an overview of tetrahydrofuran-containing marine drugs, focusing on the terpene family and related compounds. We want to offer the reader an overview of the most recent and also classic examples of tetrahydrofuran-containing terpenoids of marine origin, their isolation, biological properties, and synthetic strategies towards them. We start with some examples of fatty acids with interesting biological profiles, and then move to the broad family of terpenoid compounds (monoterpenes, sesquiterpenes, diterpenes, triterpenes, and meroterpenoids). At the end, we also highlight other small THF-containing compounds that show interesting biological activities or were recently isolated and thus have potential to show them in the near future.

2. FATTY ACIDS

2.1. C19 lipid diols

Diastereomeric *trans*-oxylipids **1**, and *cis*-oxylipid **2**, (Figure 1), were isolated in 1980 [11] and 1998 [12], respectively, from the brown alga *Notheia anomala*. Both of them display *in vitro* antihelmintic activity, inhibiting larval development in parasitic nematodes. The *trans*-isomer **1** showed similar LD_{50} values against *Haemonchus contortus* (1.8 ppm) and *Trichostrongylus colubriformis* (9.9 ppm) than commercial levamisole and closantel. Synthetic routes for these oxylipids were recently reviewed [13].

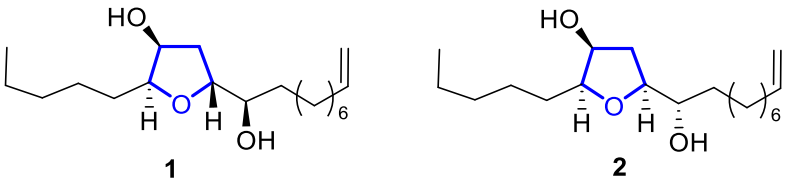

Figure 1. Structure of *trans*-oxylipid **1** and *cis*-oxylipid **2**.

2.2. Petromyroxols

In 2015, Li reported the isolation of (+)- and (-)-petromyroxols (**3**) [14]. They are oxylipids isolated from water conditioned with larval sea lamprey *Petromyzon marinus* L. Interestingly, these molecules are the first tetrahydrofuran acetogenindiols isolated from a vertebrate animal (Figure 2). **(+)-3** shows a potent olfactory response of 0.01 to 1 μM in the sea lamprey, while the (-)-isomer has a softer effect. Synthetic routes towards them were recently reviewed [13]. In 2020 Ramana and coworkers presented an update of the synthesis of **(+)-3**, along with all possible diastereoisomers [15].

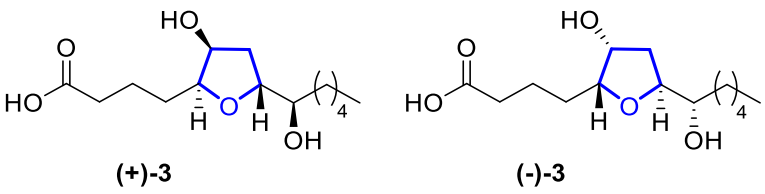

Figure 2. Structures of (+)-and (-)-petromyroxol **3**.

Preprints (www.preprints.org) | NOT PEER-REVIEWED | Posted: 21 September 2022 doi:10.20944/preprints202209.0320.v1

2.3 PMA

Petromyric acids A and B (PMA and PMB) are dehydroxylated tetrahydrofuranyl fatty acids that were isolated from larval washing extracts from the sea lamprey *Petromyzon marinus* in 2018 [16]. From the washing extract, four fatty acids related to the acetogenin family were identified: (+)-PMA (**(+)-4**), (-)-PMA (**(-)-4**), (+)-PMB (**(+)-5**), and (-)-PMB (**(-)-5**) (Figure 3).

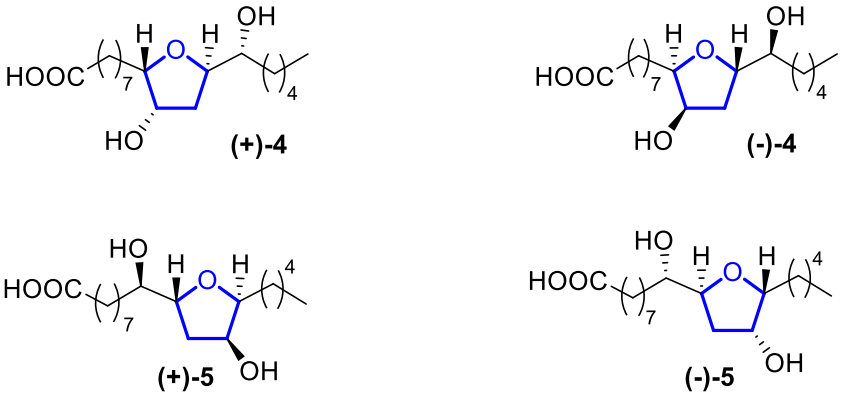

Figure 3. Structure of (+)-PMA (**(+)-4**), (-)-PMA (**(-)-4**), (+)-PMB (**(+)-5**) and (-)-PMB (**(-)-5**).

Sea lampreys are anadromous fishes that migrate, using their olfactory cues to orientate, from the ocean to freshwater to find a suitable spawning stream. When approaching river mouths, the decision of which stream is the optimal to spawn is taken using their olfactory system to detect a pheromone emitted from larval sea lampreys. When investigating larval washing extracts, four fatty acids were identified, but only **(+)-4** has proven to be the pheromone that guides lamprey adults. However, its enantiomer, **(-)-4**, does not produce the same behavioural effect. Fatty acid analogues have been reported to be pheromones in insects, but this is the first identification in fish. The sea lamprey is a destructive invader in the Laurentian Great Lakes, while in Europe its population has decreased precipitously, so **(+)-4** can be used for control and conservation of their populations.

2.4. Mutafurans

Mutafurans A-G (**6**-**12**) are brominated ene-ynetetrahydrofurans (Figure 4) that were isolated by Molinski in 2007 from themarine sponge *Xextospongia muta* [17]. Later, Liu reported the isolation of mutafuran H (**13**), a brominated ene-tetrahydrofuran isolated from sponge *Xextospongia testudinaria* within other sterols and brominated compounds[18]. Their structure and absolute configuration were determined by 1D and 2D magnetic resonance, mass spectrometry and circular dichroism.

Preprints (www.preprints.org) | NOT PEER-REVIEWED | Posted: 21 September 2022 doi:10.20944/preprints202209.0320.v1

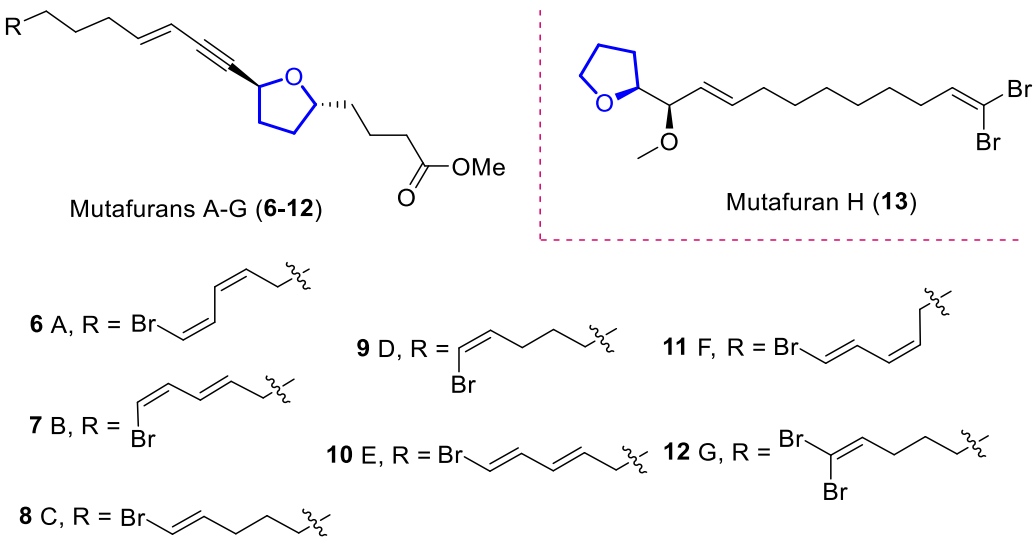

Figure 4. Structure of mutafurans A-G and the yne-lacking mutafuran H.

Mutafurans A-D showed moderate antifungal activity against the fungus *Cryptococcus neoformans var. grubii,* but were inactive against *Candida albicans* (ATCC14503 and 96-489) and *Candida glabrata* [17]. Furthermore, mutafuran H showed biological activity against *Artemia salina* larvae (LC_{50} = 2.6 μM) and a significant acetylcholinesterase inhibitory activity (IC_{50} = 0.64 μM) [18].

2.5. Aspericacids

Aspericacids A (**14**) and B (**15**) were isolated in 2020 by Ding and He from the sponge-associated *Aspergillus sp.* LS78 [19]. Both compounds bear a 2,5-disubstituted tetrahydrofuran ring coupled with an unsaturated fatty acid (Figure 5). Their structure was determined by HRESIMS, 1D and 2D NMR spectroscopy, while their absolute configuration was established relying on electronic circular dichroism (ECD). Compound**14** presents a moderate inhibitory activity against *Candida albicans* and *Cryptococcus neoformans* with a MIC value of 50 μg/mL, although **15** has a weaker activity, MIC = 128 μg/mL.

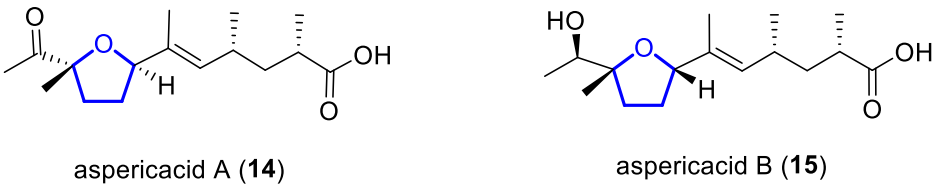

Figure 5. Structure of aspericacids A **14** and B **15**.

3. TERPENES

3.1. Monoterpenes

3.1.1.Pantofuranoids

Pantofuranoids A-F (**16-21**) are monoterpenes that were isolated in 1996 from the Antarctic red alga *Pantoneura plocamioides* [20]. They are the first monoterpenes found to contain a tetrahydrofuran moiety, and their common framework (Figure 6) suggests that they all come from the same terpene precursor.

Preprints (www.preprints.org) | NOT PEER-REVIEWED | Posted: 21 September 2022 doi:10.20944/preprints202209.0320.v1

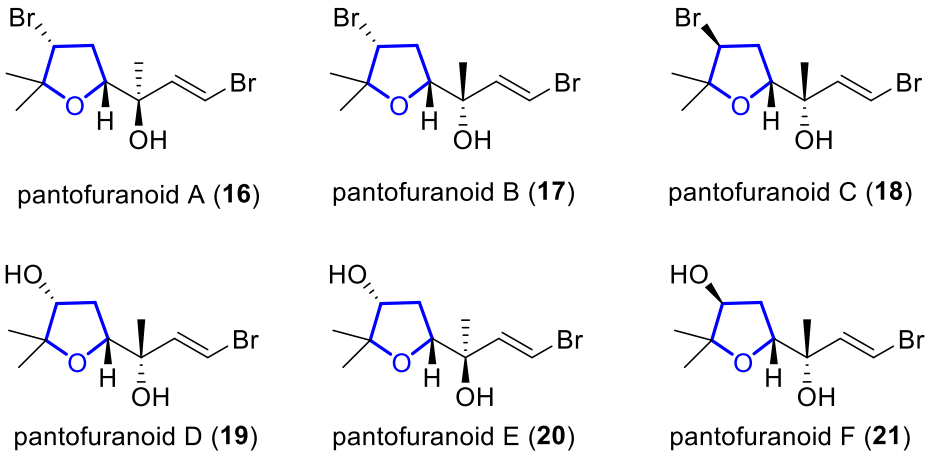

Figure 6. Proposed structure of pantofuranoids.

In 2006, Toste reported the enantioselective total synthesis of **(-)-20**, in which the key step is a vanadium-catalyzed sequential resolution/oxidative cyclization [21]. Using an *in situ* generated vanadium(V)–oxo complex with chiral tridentate Schiff base ligands as catalyst, racemic homoallylic alcohol **21** was readily converted into 2,4-*cis*-substituted THF **22** (Scheme 1). The observed stereochemistry can be explained through a chair-like transition state in wich coordination of the *pseudo*-equatorial ester group to the vanadium complex determines the selectivity of the *syn*-epoxidation step. Then, compound **22** was further elaborated to **(-)-5** in 6 steps and 29% overall yield from **22**.

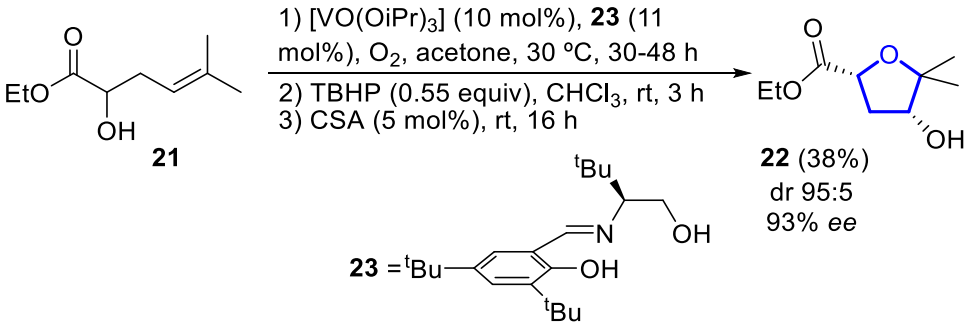

Scheme 1. Vanadium-catalyzed synthesis of the tetrahydrofuranyl core of (-)-pantofuranoid E by Toste.

3.1.2.Furoplocamioids

Furoplocamioids A-C **24-26** (Figure 7) are monoterpenes that were isolated in 2001 from the red marine alga *Plocamium cartilagineum* [22]. They bear an unusual polyhalogenated tetrahydrofuranyl ring. Their structural similarity to pantofuranoids suggests a close relationship between the species that produce them. This is an interesting fact, since *Plocamium cartilagineum* and *Pantoneura plocamioides* are classified in different orders, Gigartinales and Ceramiales. Therefore, a taxonomic revision could be required. Later, Darias group determined the C7 relative stereochemistry by comparison with the NMR spectra of similar reported terpenes [23]. González-Coloma and coworkers found that **24** and **26** show antifeedant effects against *Leptinotarsa decemlineata*. **26** was also an efficient aphid repellent (against *Mizuspersicae* and *Ropalosiphumpadi*) and selective insect cell toxicant. In addition, both compounds showed low mammalian toxicity and phytotoxic effects [24].

Preprints (www.preprints.org) | NOT PEER-REVIEWED | Posted: 21 September 2022 doi:10.20944/preprints202209.0320.v1

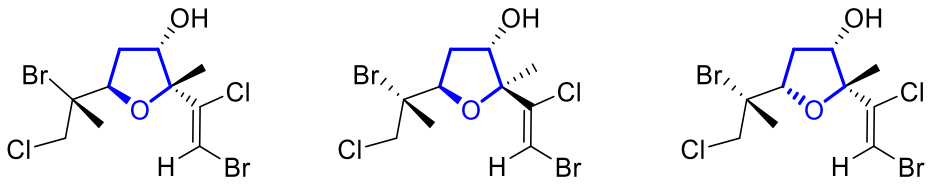

Figure 7. Structure of furoplocamioids A-C (**24**-**26**).

3.2. Sesquiterpenes

3.2.1.Heronapyrrol D

Heronapyrrols A-C are pyrroloterpenes that were isolated in 2010 from a marine *Streptomyces* sp. CMB-M0423 [25]. They present bioactivity against Gram-positive bacteria *Staphylococcus aureus* ATCC 9144 and *Bacillus subtilis* ATCC 6633 but no mammalian cytotoxicity. Heronapyrrol C (**27**), apart from the characteristic and unusual 2-nitropyrrol moiety of this family, presents a bis-tetrahydrofuran core. Later, Capon and Stark first synthesized and then isolated heronapyrrol D (**28**) (Figure 8) from the same marine-derived microbe [26]. Heronapyrrol D displays bioactivity against Gram-positive bacteria *Staphylococcus aureus* ATCC 25923 (IC_{50} = 1.8 μM), *Staphylococcus epidermidis* ATCC 12228 (IC_{50} = 0.9 μM) and *Bacillus subtilis* ATCC 6633 (IC_{50} = 1.8 μM). It is though inactive against the Gram-negative bacteria *Pseudomonas aeruginosa* ATCC 10145 and *Escherichia coli* ATCC 25922.

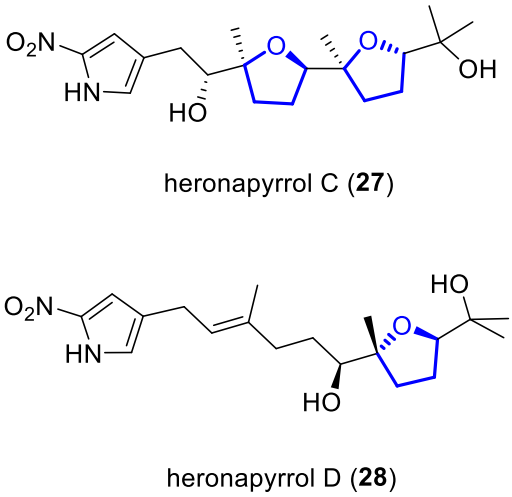

Figure 8. Structure of (+)-heronapyrrol C (**27**) and (+)-heronapyrrol D (**28**).

To determine the relative and absolute stereochemistry of **(+)-27**, Stark and coworkers proposed and synthesized the most likely stereostructure of its enantiomer **(-)-27**, based on a biomimetic polyepoxide cyclization [27]. The same author also reported the preparation of a bioisosteric carboxylate analog of **(-)-27** [28].

The first total synthesis of **(+)-27** was reported in 2014 by Brimble and coworkers, who used as key steps to introduce the 5 stereogenic centers a Julia-Kocienski coupling, a Shi epoxidation and a catalytic epoxide opening reaction [29]. The same year, the first total synthesis of **(+)-28** was achieved by Capon and Stark using a similar approach [26]. Brimble and Furkert reviewed in 2016 the isolation and synthesis of these family of compounds [30].

Later on, the same authors reported another total synthesis for both **(+)-27** and **(+)-28** [31]. Shi epoxidation of diol **29**, followed by CSA-catalysed epoxide opening and cyclization, produces diastereomerically pure **30** in 75% yield over two steps. Further 8 steps, with 31% yield over them, produces intermediate **31**, which deprotection gives

Preprints (www.preprints.org) | NOT PEER-REVIEWED | Posted: 21 September 2022 doi:10.20944/preprints202209.0320.v1

(+)-heronapyrrol D (**28**). Epoxidation of **28** with Shi ketone catalyst, followed by CSA catalyzed epoxide opening, produces enantiomerically pure (+)-heronapyrrol C (**27**) in 75% yield (Scheme 2).

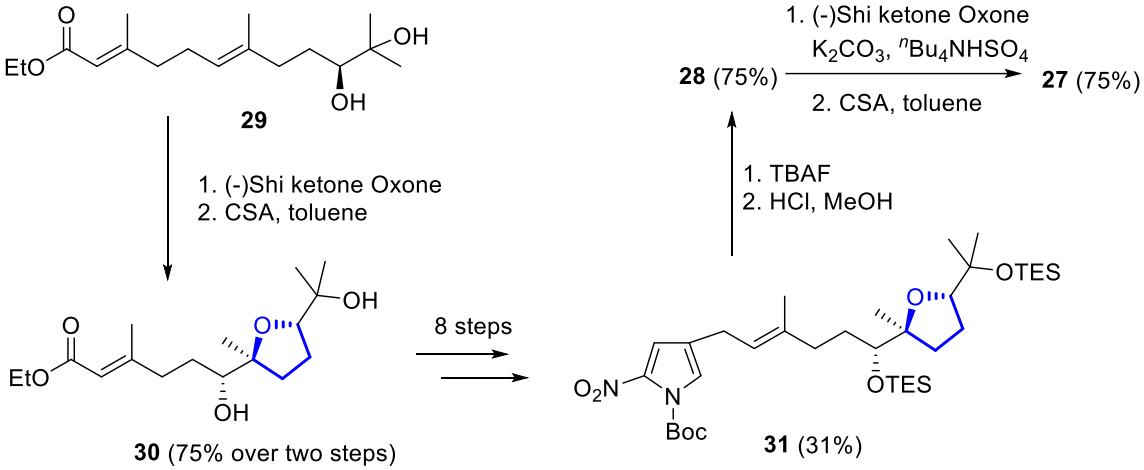

Scheme 2. Synthesis of (+)-heronapyrrol C (**27**) and (+)-heronapyrrol D (**28**).

Other synthetic approaches towards the 2-nitropyrrole system have been investigated by Brimble and Furkert, finding that sonogashira coupling of 4-iodo-2-nitropyrrole with the appropriate alkyne was more effective than an approach relying on Stille coupling [32].

3.2.2.Kumausallene and kumausyne

(-)-Kumausallene (**32**) was isolated in 1983 from the marine red alga *Laurencia nipponica* Yamada [33]. This compound belongs to a family of non-isoprenoid sesquiterpenes that contain a 2,6-dioxa-bicyclo[3.3.0]octane core with an *exo*-cyclic bromoallene (Figure 9).

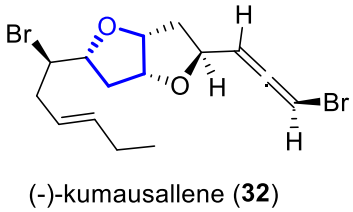

Figure 9. Structure of kumausallene.

In 1993 the first total synthesis of **(±)-32** was reported by Overman, who chose a hexahydrobenzofuranone **33** (obtained by a Prins cyclization-pinacol rearrangement from **34**) as the key intermediate for the construction of the bis-tetrahydrofuran unit. Further transformation of **33** into bicyclic lactone **35** (within 3 further steps) and final methanolisis and tandem cyclization of the corresponding hydroxyester provided in good yield the desired dioxabicyclo[3.3.0]octane **36** [34].

Preprints (www.preprints.org) | NOT PEER-REVIEWED | Posted: 21 September 2022 doi:10.20944/preprints202209.0320.v1

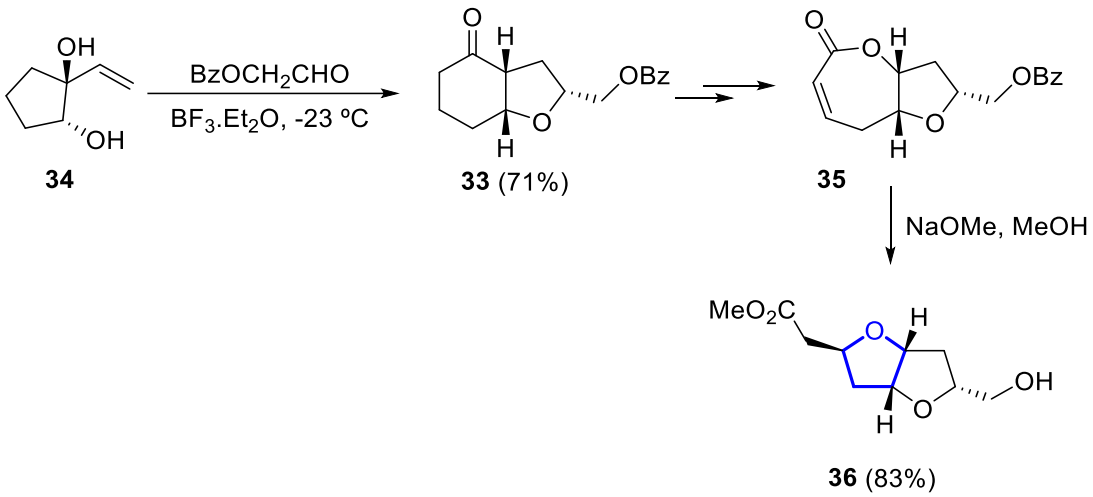

Scheme 3. Synthesis of the dioxabicyclo[3.3.0]octane unit of(±)-kumausallene (**32**) by Overman.

In 2011, a synthetic approach for **(-)-32** by Tang employed a desymmetrization strategy for the formation of the 2,5-*cis*-substituted THF ring [35]. C_2-symmetric diol **37** is desymmetrised by a palladium-catalysed cascade reaction to form lactone **38** in 87% yield (Scheme 4). The total synthesis comprised just 12 steps from commercial acetylacetone. Ramanaet al. published in 2015 a different formal total synthesis of **(-)-32** based on a chiral pool approach [36].

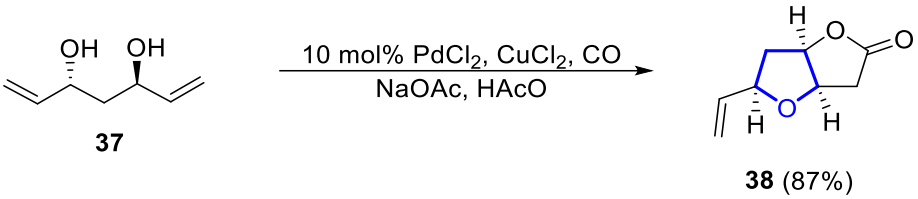

Scheme 4. Synthesis of the tetrahydrofuranyl ring of (-)-**32** through desymmetrization by Tang.

(+)-*trans*-Kumausyne (**39**) (Figure 10) is an halogenated non-isoprenoid sesquiterpene isolated in 1983 from red alga *Laurencia nipponica* Yamada [37]. Its first total synthesis was achieved in 1991 by Overman and coworkers [38]. A review covering the synthetic approaches towards kumausallene and kumausyne, and other natural products containing a 2,3,5-trisubstituted tetrahydrofuran moiety, was published by Fernandes in 2020 [13].

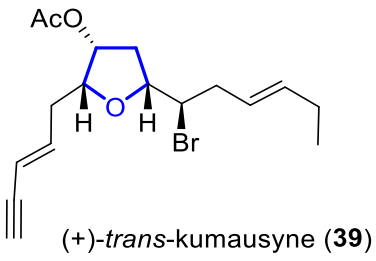

Figure 10. Structure of (+)-*trans*-Kumausyne (**39**).

3.3. Diterpenes

3.3.1.Darwinolide

(+)-Darwinolide (**40**) (Figure 11) is a diterpene isolated in 2016 by Baker from the Antartic Dendroceratid sponge *Dendrillamembranosa* [39]. It presents 4-fold selectivity against a biofilm phase of methicillin-resistant *Staphylococcus aureus* (IC_{50} of 33.2µM),

Preprints (www.preprints.org) | NOT PEER-REVIEWED | Posted: 21 September 2022 doi:10.20944/preprints202209.0320.v1

compared to the planktonic phase (with the higher MIC of 132.9 μM). This interesting property and its low mammalian cytotoxicity (IC_{50} of 73.4 mM) against a J774 macrophage cell line, turns darwinolide into a possible scaffold for antibiofilm-specific antibiotics. Additionally, it was found to have modest activity (11.2 μM) against *L. donovani*-infected macrophages [40].

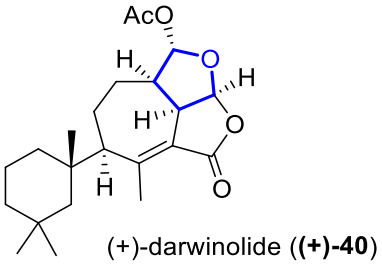

Figure 11. Structure of darwinolide.

Its total synthesis was reported in 2019 by Christmann [41]. The required tetrahydrofuranyl ring is installed starting from the commercially available anhydride **41**, that is converted to the 2,5-dimethoxylated tetrahydrofuran **42** in four steps. A sequence of oxidation (with o-iodoxybenzoic acid), saponification and Criegee oxidation with $Pb(OAc)_4$ is then used to convert **42** into **43** in 61% yield over three steps (Scheme 5). Further 14 linear steps are needed to complete the total synthesis of **40**, with an overall yield of 1.4%.

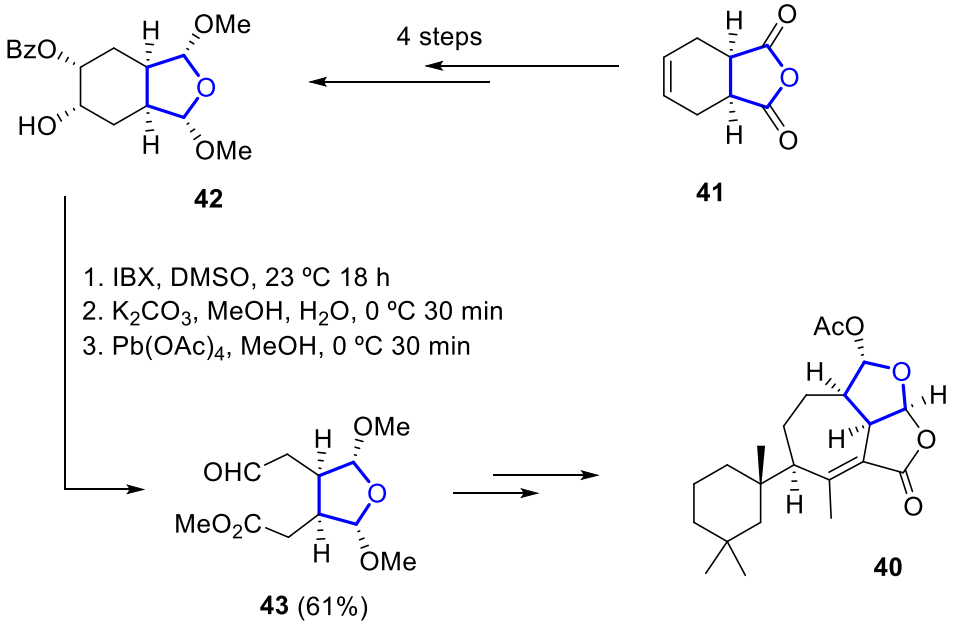

Scheme 5. Synthesis of the key THF containing intermediate in Christmann's total synthesis of darwinolide.

3.3.2 Uprolides

Cembranolides are a family of compounds related to cembrene, which is a 14-membered macrocyclic diterpene with multiple (*E*)-double bonds. Among them, uprolides are a subfamily of compounds named after the University of Puerto Rico. Uprolides A-G were isolated in 1995 by Rodríguez and coworkers from the Caribbean gorgonian *Eunicea Mammosa* and their structure was assigned by spectroscopic methods and chemical interconversion [42, 43]. They are the first natural cembranolides from a Caribbean gorgonian that bear a double bond at C6 or C8. While Uprolides A-C show an epoxy moiety, Uprolides D-G seemed to contain a tetrahydrofuran moiety instead. Uprolides D (**44**), D acetate (**45**), D diacetate (**46**) and E acetate (**47**) (Figure 12) present a

Preprints (www.preprints.org) | NOT PEER-REVIEWED | Posted: 21 September 2022 doi:10.20944/preprints202209.0320.v1

moderate cytotoxicity against HeLa cells ((IC$_{50}$=2.5 to 5.1 μg/ ml). Moreover, **45** shows cytotoxicity against the following human tumor cell lines: CCRF-CEM T-cell leukemia (IC$_{50}$=7.0 μg/ml), HCT 116 colon cancer (IC$_{50}$=7.0 μg/ml), and MCF-7 breast adenocarcinoma (IC$_{50}$=0.6 μg/ml).

Later structural revisions determined the presence of a tetrahydropyran ring, instead of the previously proposed tetrahydrofuran, in Uprolides F-diacetate and G-acetate, hypotheses that were confirmed by asymmetric total synthesis of these natural products [44-47].

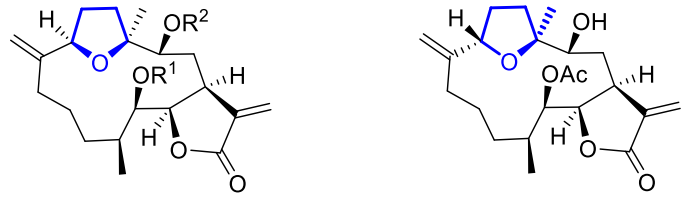

Uprolide D **44** $R^1 = R^2 = H$
Uprolide D acetate **45** R^1 = Ac, R^2 = H
Uprolide D diacetate **46** $R^1 = R^2$ = Ac

Uprolide E acetate **47**

Figure 12. Structure of tetrahydrofuran-containing members of the uprolide family.

In 2007, a synthetic approach to obtain the macrocyclic core of **44** was proposed by Ramana [48]. The formation of the macrocyclic core is produced by ring closing metathesis (RCAM) using a Grubbs' first generation catalyst. The RCAM of acetate **48** produces 13-membered macrocyclic **49** in 67% yield (Scheme 6). The macrocyclic core of uprolide E could not be synthesized using the same methodology.

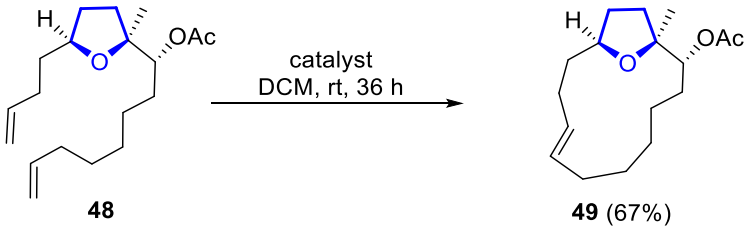

48 **49** (67%)

Scheme 6. Synthesis of macrocyclic core of uprolide D by Ramana.

Marshall developed a synthetic route for C1/C14 bis-epimer of **44** in which the macrocyclization is produced by an intramolecuar Barbier reaction [49]. Some years later, other members of the uprolide family, which lack the tetrahydrofuran ring, have been isolated from the gorgonian octocoral *Eunicea succinea* [50].

3.4. Triterpenes

3.4.1.Intricatetraol

Intricatetraol (**50**) is a halogenated triterpenoid with a C_2 symmetry that was isolated in 1993 from the red alga *Laurencia intricata*. Suzuki and coworkers observed that a crude fraction of the extract showed cytotoxic activity against P388 leukemia cells with an IC$_{50}$ value of 12.5 μg/mL. Nevertheless, pure intricatetraol was not longer active after chromatography. At first, its stereostructure was proposed being based on its hypothetical biogenesis [51]. In 2006, Morimoto confirmed this assignment by synthesizing a degradation product of intricatetraol through a two-directional synthesis [52].

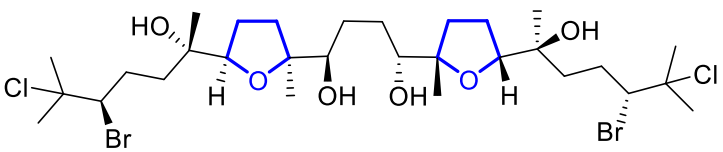

intricatetraol **50**

Preprints (www.preprints.org) | NOT PEER-REVIEWED | Posted: 21 September 2022 doi:10.20944/preprints202209.0320.v1

Figure 13. Structure of (+)-intricatetraol **50**.

One year later, Morimoto completed the asymmetric total synthesis of **(+)-50** and thus determined its absolute configuration [53]. The tetrahydrofuran ring **51** is stereospecifically constructed by treatment of diepoxyalcohol **52** with lithium hydroxide aqueous solution. Further 10 steps (with an accumulated yield of 30%) are needed to obtain intermediate **53**, which is then dimerised to afford **54** by olefin metathesis with a second generation Grubbs catalyst. Final diimide reduction of intermediate **54** produces **(+)-50** (Scheme **7**).

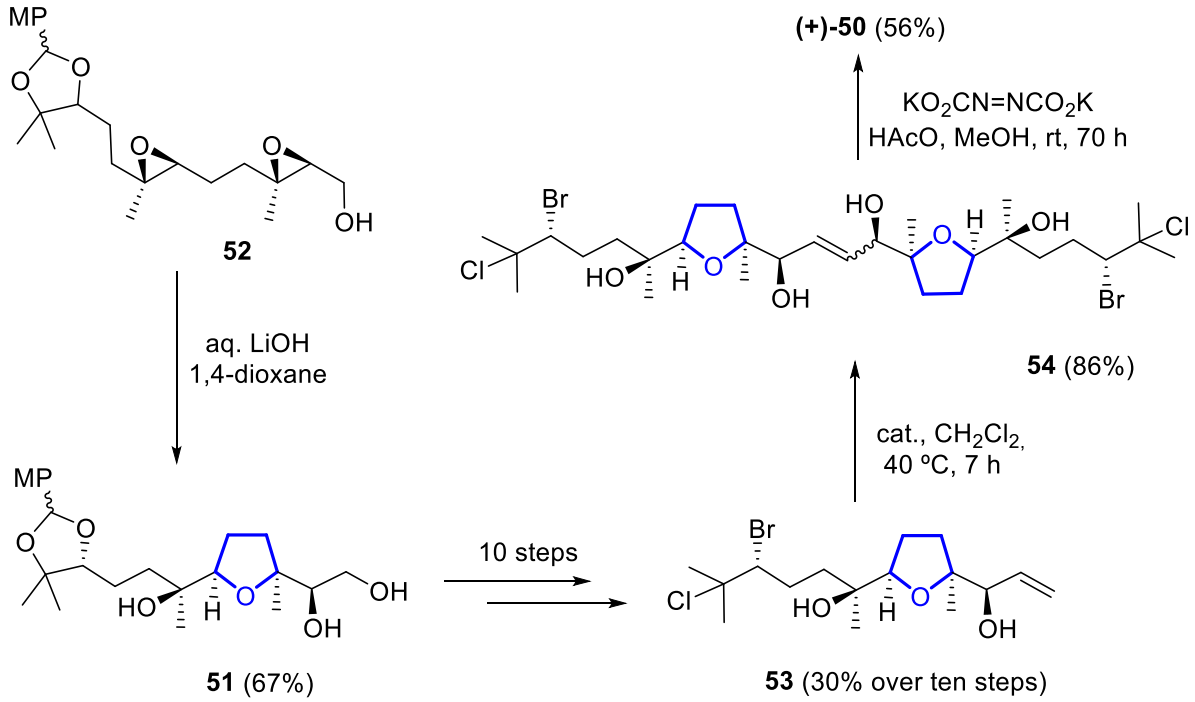

Scheme 7. Synthesis of of (+)-intricatetraol (**(+)-50**).

3.4.2. Omaezakianol

Omaezakianol (**55**) is a squalene-derived triterpene polyether that was isolated in 2008 from the red alga *Laurencia omaezakiana* by Morimoto and coworkers [54]. The same group rapidly reported its first asymmetric total synthesis and therefore stablished its absolute configuration [55]. Key steps were olefin cross metathesis and an epoxide-opening cascade.

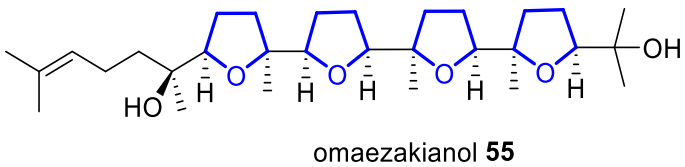

Figure 14. Structure of (+)-omaezakianol (**55**).

In 2010, Corey reported a short total synthesis via a biomimetic epoxide-initiated cationic cascade reaction [56]. Compound **56** is treated with camphorsulfonic acid (CSA) to induce the epoxide-opening cascade cyclization, producing **57**. Reduction of **57** with sodium in acetone under reflux, forms the terminal double bond with opening of the THF ring, affording **55** in 76% yield (Scheme 8). The synthesis was thus accomplished in just six steps from squalene.

Preprints (www.preprints.org) | NOT PEER-REVIEWED | Posted: 21 September 2022 doi:10.20944/preprints202209.0320.v1

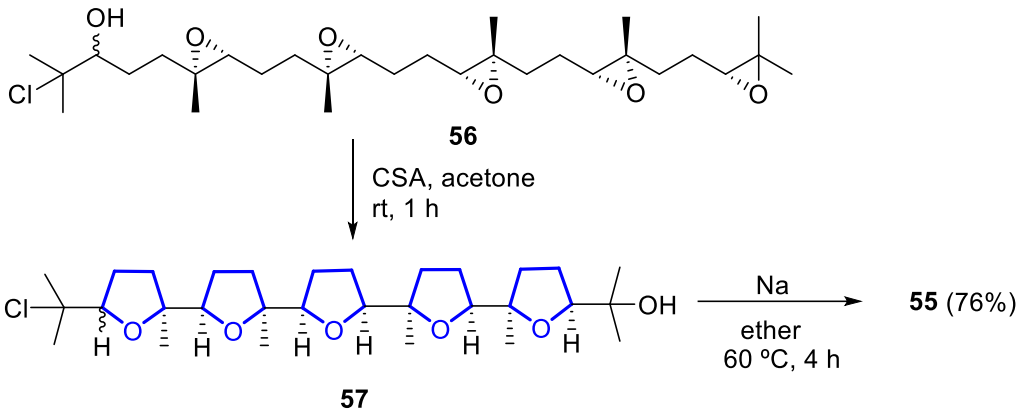

Scheme 8. Synthesis of (+)-omaezakianol **55** by Corey via an epoxide-initiated cationic cascade.

Another biomimetic epoxide-opening cascade for the synthesis of **(+)-55** was reported in 2013 by Morimoto and coworkers [57]. The cascade, that mimics the direct hydrolysis mechanism of epoxide hydrolases, goes by 5-*exo* tandem cyclization of the terminal epoxide triggered by Brønsted acid-catalysis. Intermediate **58** undergoes an epoxide-opening cascade reaction with TfOH to afford **(+)-55** in 33% yield (Scheme 9).

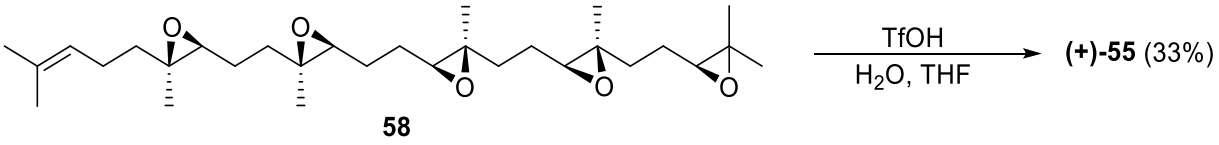

Scheme 9. Synthesis of (+)-omaezakianol (**(+)-55**) by a biomimetic epoxide-opening cascade.

3.4.3. Longilenes

Longilenes are triterpene polyethers that were first isolated from the wood of *Eurycoma longifolia* in the form of (-)-longilene peroxide (**(-)-59**) [58, 59]. In 2001, Morimoto accomplished its total synthesis [60] and determined its absolute configuration. The same author also developed a biomimetic synthesis of the C9-C16 fragment of oxasqualenoids in an enantioselective manner [61]. This chiral building block could be used as an advanced intermediate for the synthesis of different polyethers, such as teurilene, longilene peroxide or glabrescol.

In 2018, Fernández and Daranas reported the isolation of other members of the family, namely (+)-longilene peroxide (**(+)-59**), longilene (**60**) and the derivative (+)-prelongilene (**(+)-61**) from the red seaweed *Laurencia viridis* [62]. These compounds present Ser-Thr protein phosphatase 2A inhibitory activity (Figure 15). To date, no synthetic approaches have been reported.

Preprints (www.preprints.org) | NOT PEER-REVIEWED | Posted: 21 September 2022 doi:10.20944/preprints202209.0320.v1

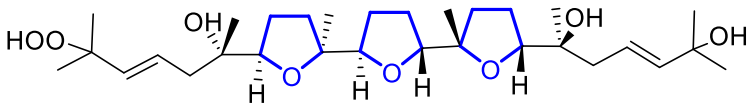

(-)-longilene peroxide (**(-)-59**)

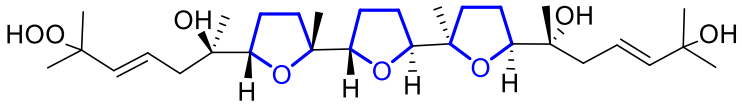

(+)-longilene peroxide (**(+)-59**)

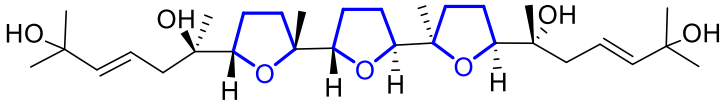

longilene (**60**)

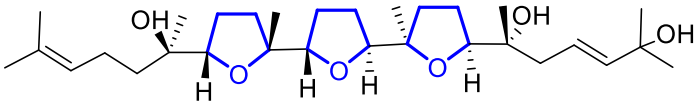

(+)-prelongilene (**(+)-61**)

Figure 15. Structure of (-)-longilene peroxide (**(-)-59**), (+)-longilene peroxide (**(+)-59**), longilene (**60**) and the derivative (+)-prelongilene (**(+)-61**).

3.4.4. Laurokanols and yucatecone

In 2021, laurokanols A-E (**62-66**) and yucatecone(**67**) (Figure **16**), polyether triterpenes, were isolated from the red alga *Laurencia viridis* [63]. Laurokanols have an unprecedented tricyclic core with an [6,6]-spiroketal system. Yucatecone is the first compound of this series with an *R* configuration at the C14 position. A biogenetic model, supported by DFT calculations, was then postulated for the biogenesis of yucatecone.

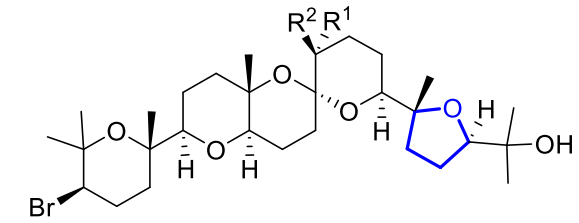

Laurokanol A **62**: R^1 = Me, R^2 = H
Laurokanol B **63**: R^1 = CH_2Cl, R^2 = OH
Laurokanol C **64**: R^1 = OH, R^2 = CH_2Cl
Laurokanol D **65**: R^1 = OH, R^2 = CH_2Br

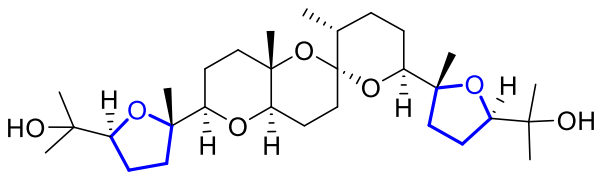

Laurokanol E (**66**)

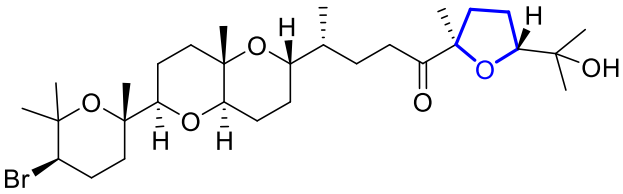

Yucatecone (**67**)

Figure 16. Structures of laurokanols A-E (**62-66**) and yucatecone (**67**).

Preprints (www.preprints.org) | NOT PEER-REVIEWED | Posted: 21 September 2022 doi:10.20944/preprints202209.0320.v1

3.4.5. Thyrsenol

Thyrsenol A (**68**) and B (**69**) (Figure 17) are polyether squalene derivatives that were isolated by Norte and coworkers in 1997 from the red alga *Laurencia viridis* [64]. Although both compounds show high activity against murine lymphoid neoplasm P-388 cells, compound **69** induced significantly higher inhibitory effects [65]. Other related compounds, like thyrsiferol derivatives and dehydrovenustatriol were found to be even more active. Therefore, it was postulated that the presence of a flexible chain around C14 to C19, and its configuration, are of particular importance for the bioactivity of these compounds. Later, Fernández and coworkers have also found **69** to have protein phosphatase PP2A inhibitory activity [66]. The activity was comparable to that of dehydrothyrsiferol and thysiferyl-23-acetate, concluding that a hydroxyl group at C15 or C16 is a key factor for their intrinsic activity. In 2011, the isolation of other derivatives has been reported [67].

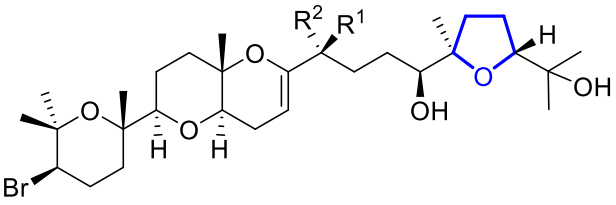

Thyrsenol A (**68**): R^1 = OH, R^2 = CH_2OH
Thyrsenol B (**69**): R^1 = CH_2OH, R^2 = OH

Figure 17. Structure of thyrsenol A (**68**) and B (**69**).

3.4.6. Saiyacenol

Saiyacenols A (**70**) and B (**71**) (Figure **18**) are triterpene polyethers that were isolated in 2012 from the red alga *Laurencia viridis*. Both inhibit cell proliferation of various human tumour cell lines (MM144 (human multiple myeloma), HeLa (human cervical carcinoma), CADO-ES1 (human Ewing's sarcoma), showing the best inhibitory activity against Jurkat (human T-cell acute leukaemia) [68]. In 2015, saiyacenol C (**72**), and two hydroxylated derivatives **73** and **74**, were isolated from the same alga [69]. Although saiyacenols showed no activity toward a range of bacteria and fungal strains, compounds **71** and **72** avoid *Navicula* cf. *salinicola* and *Cylindrotheca* sp. growth, while compounds **73** and **74** were also active against germination of *Gayraliaoxysperma*.

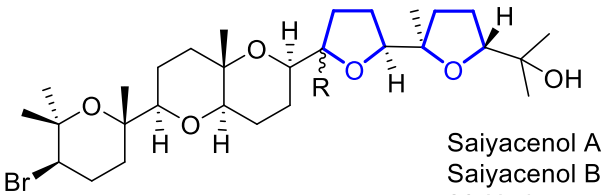

Saiyacenol A (**70**): R = CH_3; 15S*
Saiyacenol B (**71**): R = CH_3; 15R*
28-Hydroxysaiyacenol A (**73**): R = CH_2OH; 15S*
28-Hydroxysaiyacenol B (**74**): R = CH_2OH; 15R*

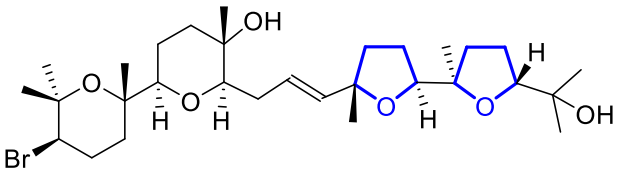

Saiyacenol C (**72**)

Figure 18. Structure of saiyacenols A-C (**70-72**) and their hydroxylated derivatives**73** and **74**.

More recently, Piñero and Fernández evaluated a range of natural and semisynthetic terpenoid polyethers against protozoan parasites of the *Trypanosoma* and *Leishmania* genera [70]. Both **70** and **71** have anti-protozoal activity against *Leishmania amazonensis*

Preprints (www.preprints.org) | NOT PEER-REVIEWED | Posted: 21 September 2022 doi:10.20944/preprints202209.0320.v1

(IC_{50} = 12.96 and 10.32 µM, respectively). Interestingly, saiyacenolA **70** was also effective against the highly resistant *Trypanosoma cruzi* (IC_{50} = 13.75 ± 2.28 µM). The semisynthetic 28-iodosaiyacenol B showed a high value (IC_{50} = 5.40 ± 0.13 µM) against *Leishmania amazonensis* and no toxicity to murine macrophage J774.A1. This turns it into a possible scaffold for antikinetoplastid drugs, as the data are comparable to those of the reference drug miltefosine (IC_{50} = 6.48).

Very recently, Nishikawa and Morimoto reported the asymmetric total synthesis of Saiyacenol A, along with that of the related Aplysiol B [71]. There, an epoxide opening cascade was used to form both THF rings in the same step. Thus, from advanced precursor **75**, treatment with CSA provoked two sequential 5-*exo* openings to form the oxygenated rings in bis-tetrahydrofuran **76**. Last step consisted on cross-methathesis with the ruthenium catalyst **77** and later bromoetherification with BDSB. Preliminary cytotoxicity was tested against P388, HT-29 and HeLa tumor cell lines, showing values of 5.4, 85 and >100 µM, respectively.

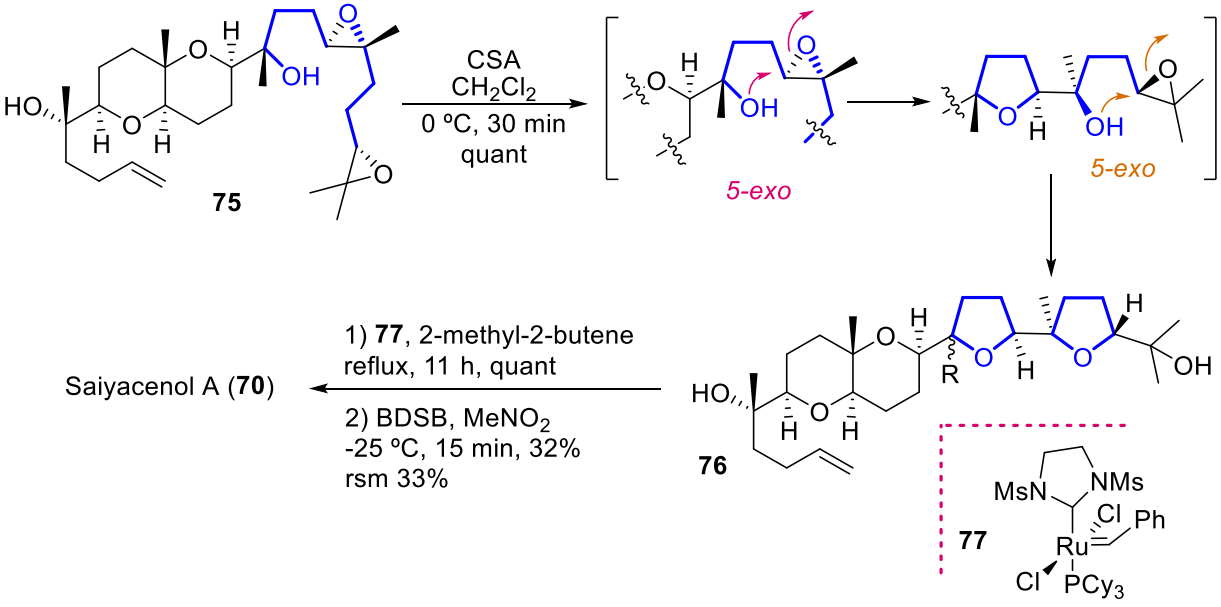

Scheme 10. Synthesis of saiyacenol A by Nishikawa and Morimoto.

3.4.7. Teurilene

Teurilene (**78**) (**Figure 19**) is a triterpene polyether that was isolated in 1985 from the red alga *Laurencia obtusa* by Kurosawa and coworkers [72]. It has three linked 2,5-disubstituted THF rings and, even though it has eight stereogenic centres, it is an achiral compound due to its *meso* symmetry (C_s). Compound **78** has a remarkable cytotoxic activity against KB cells (IC_{50} = 7.0 µg mL^{-1}) [59]. Synthetic approaches and routes up to 2014 are commented in a previous review [73].

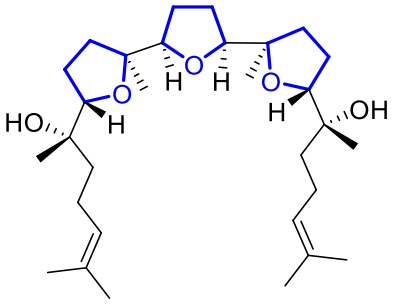

Figure 19. Structure of teurilene **78**.

3.4.8. Thyrsiferol

Preprints (www.preprints.org) | NOT PEER-REVIEWED | Posted: 21 September 2022 doi:10.20944/preprints202209.0320.v1

Thyrsiferol (**79**) is a polyoxygenated triterpenoid ether that was isolated in 1978 from the red alga *Laurencia thyrsifera* [74]. Its absolute stereochemistry (**Figure 20**) was determined in 1986 when venustatriol was isolated, since the latter could be crystallized and characterized by X-ray diffraction [75]. During the next two decades, a plethora of thyrsiferol derivatives have been isolated. Their biological profiles (cytotoxic, anti-viral, anti-tumor) have attracted much attention and several syntheses were published and reviewed in 2008 [76].

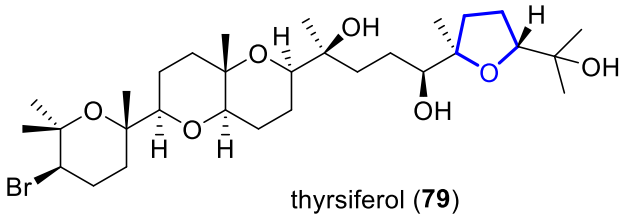

thyrsiferol (**79**)

Figure 20. Structure of thyrsiferol(**79**).

Thyrsiferol has later been found to inhibit hypoxia-induced hypoxia-inducible factor-1 (HIF-1) activation in T47D human breast tumor cells, as well as to inhibit a mitochondrial ETC complex I and show tumor cell line-selective time-dependent inhibition of cell viability/proliferation [67]. In addition, Piñero and Fernández recently reported it to be active against *Acanthamoeba castellanii* trophozoites (IC_{50} = 13.97 μM). Its derivative, 22-hydroxydehydrotyrsiferol was similarly active (IC_{50} = 17.00 μM), and both were not toxic against murine macrophages, which makes them potential leads for the discovery of novel amoebicidal substances [77].

3.4.9.Rhabdastins

The first members of this family, RhabdastinsA-G, were first isolated in 2010 by Iwagawa from the sponge *Rhabdastrellaglobostellata* [78]. They belong to the group ofisomalabaricane triterpenes. In 2021, the tetrahydrofuran-containing rhabdastins H (**80**) and I (**81**) (Figure 21) were isolated from the sponge *Rhabdastrella* sp. [79]. They are the first marine isomalabaricanes which present a tetrahydrofuran unit in their structure. Both compounds show antiproliferative effect against K562 (IC_{50} 11.7 and 9.8 μM, respectively) and Molt4 (IC_{50} 16.5 and 11.0 μM) leukemic cells.

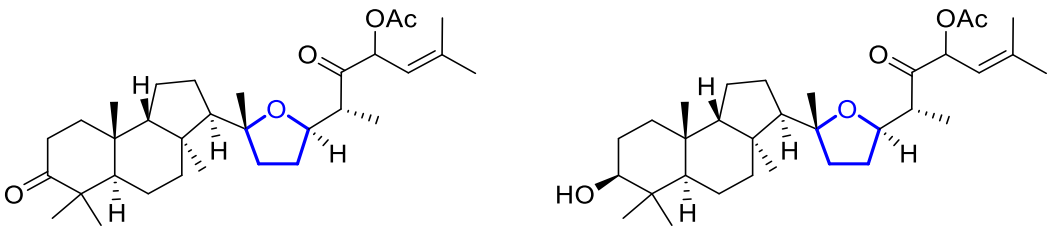

rhabdastin H (**80**) rhabdastin I (**81**)

Figure 21. Structure of rhabdastins H (**80**) and I (**81**).

3.5. Meroterpenes

3.5.1.Alisiaquinones and alisiaquinol

Alisiaquinones A-C (**82-84**) and alisiaquinol (**85**) (Figure **22**) are meroterpenes that were isolated in 2008 from a New Caledonian deep water sponge [80]. They display mild antimalarial activity, but the high level of toxicity (100% and 80% mortality, respectively) showed in vivo assays limited their interest as antimalarial agents. Nevertheless, their structure can be an inspiration for the development of related structures towards novel antimalarial drugs.

Preprints (www.preprints.org) | NOT PEER-REVIEWED | Posted: 21 September 2022 doi:10.20944/preprints202209.0320.v1

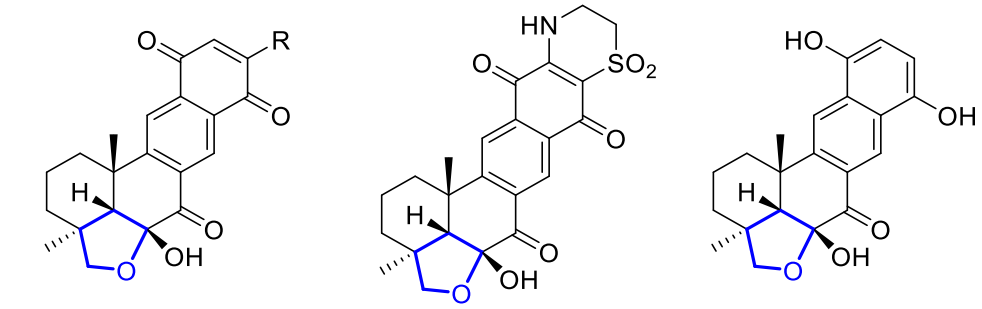

Figure 22. Structure of alisiaquinones A-C (**82**-**84**) and alisiaquinol (**85**).

3.5.2.Tricycloalterfurenes

Tricycloalterfurenes A-D (**86**-**89**) were isolated in 2017 from the culture extract of an *Alternaria alternata* strain (k21-1) isolated from the surface of the marine red alga *Lomentaria hakodatensis* [81]. These meroterpenes present activity against three phytoplankton (*Chattonella marina*, *Heterosigma akashiwo*, and *Prorocentrum donghaiense*), and one marine zooplankton (*Artemia salina*). The higher activity of tricycloalterfurene A (64, 37, 46% respectively against the phytoplankton species) indicates that hydroxylation at C2 or C3 negatively influences the activity against these organisms. Later, Oh and Shin reported the isolation, from a marine-derived *Stemphylium* sp. fungus, of tricycloalterfurenes E-G (**90**-**92**) [82]. Very recently, Fraga proposed some structural revisions [83]. Regarding tricycloalterfurenes A-C, the correct configuration of the hydroxyl group would be *4R* (Figure **23**), comparing the NMR data with that of guignardone T [84]. With respect to trycicloalterfurenes D, the correct configuration was proposed to be 6-β-OH (*6R*), also by NMR data comparison to similar systems [85]. To date, no synthetic approaches have been reported.

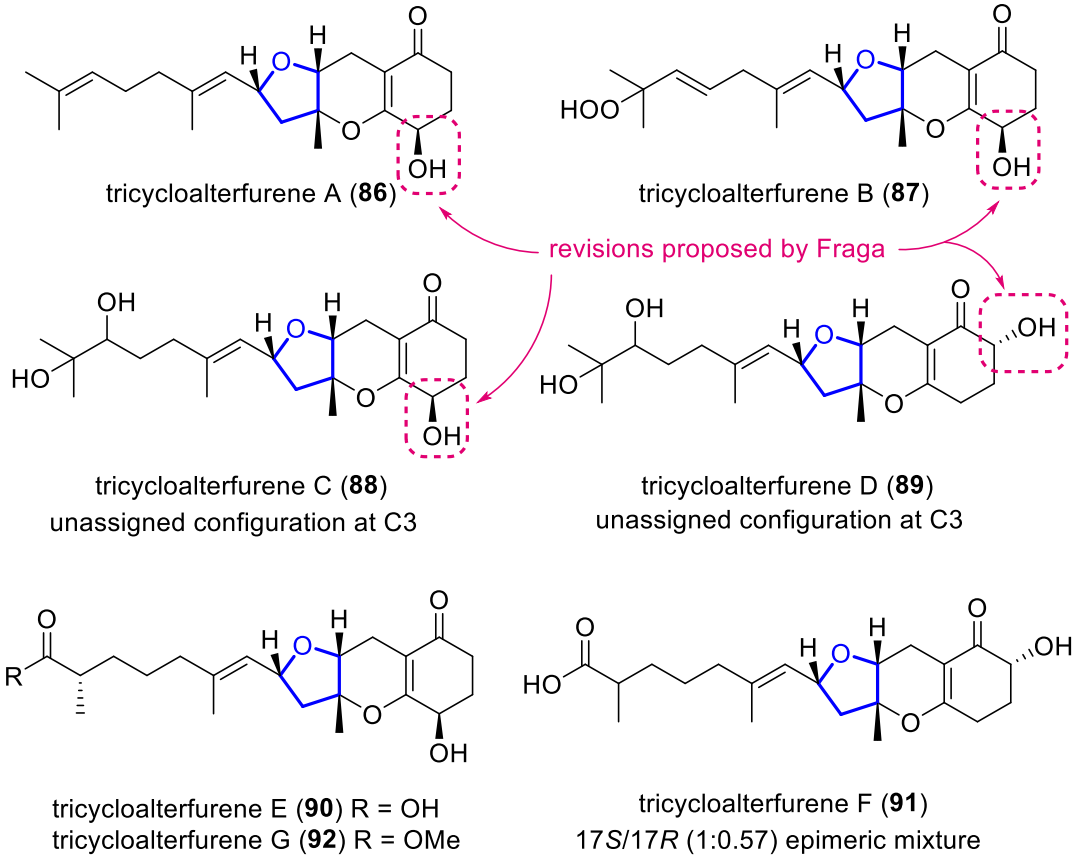

Preprints (www.preprints.org) | NOT PEER-REVIEWED | Posted: 21 September 2022 doi:10.20944/preprints202209.0320.v1

Figure 23. Structure of tricycloalterfurenes and proposed structural revisions (in pink) by Fraga.

3.5.3.Marinoterpins

Marinoterpins A-C (**93-95**) (**Figure 24**) are linear merosesterterpenoids that were recently isolated (2021) by Winter and Fenical from the marine-derived actinomycete bacteria *Streptomyces* sp. AJS-327 and CNQ-253 [86]. Due to their similarity to theaurachin family of compounds, amarinoterpin biosynthetic cluster (*mrt*) was identified. Thus, a biosynthetic route for the 3-geranylfarnesyl-2-methylquinoline core was proposed, although the reactions that lead to the tetrahydrofuran rings as well as the N-oxidation still remain unknown.

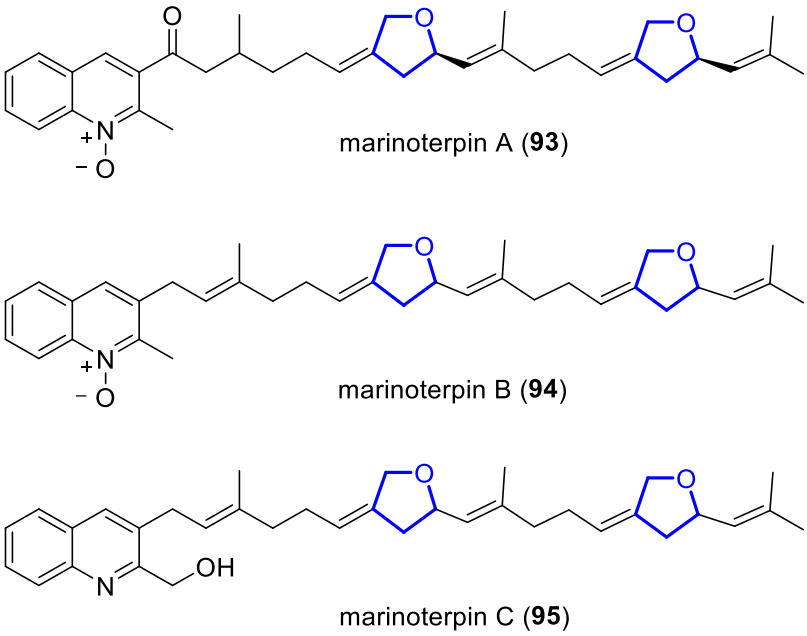

Figure 24. Structure of marinoterpins A-C (**93-95**).

4. OTHER TETRAHYDROFURAN DERIVATIVES

4.1. Substituted tetrahydrofurans

4.1.1.Pachastrissamine (Jaspine B)

Pachastrissamine (**96**), was first isolated by Higa and coworkers from a marine sponge of the genus *Pachastrissa* [87]. A year later, Debitus reported its isolation from another sponge *Jaspis* sp. and thus named the compound jaspine B [88]. Other related compounds were also isolated, namely jaspine A (**97**) (Figure **25**). Pachastrissamine is a sphingolipid, in particular a derivative from anhydrophytosphingosine. Its biological activity and synthetic endeavors until 2016 were summarized by Martinková in a mini review [89].

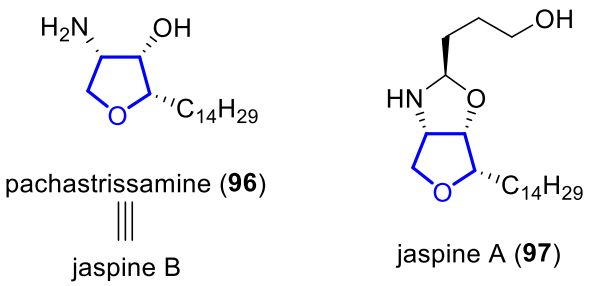

Figure 25. Structures of pachastrissamine (jaspine B, **96**) and jaspine A (**97**).

4.1.2.Myrothecols

Preprints (www.preprints.org) | NOT PEER-REVIEWED | Posted: 21 September 2022 doi:10.20944/preprints202209.0320.v1

In 2020, (-)-1*S*-myrothecol (**(-)-98**), (+)-1*R*-myrothecol (**(+)-98**) and methoxy-myrothecol (**99**) (Figure 26), were isolated from deep-sea fungus *Myrothecium sp.* BZO-L062 [90]. Enantiomers **(-)-98** and **(+)-98** were separated by normal-phase chiral HPLC, and their absolute configurations were established by ECD spectra. Compounds **(-)-98** and **(+)-98** display anti-inflammatory activity, inhibit nitric oxide formation in lipopolysaccharide-treated cells (RAW264.7), and present antioxidant activity in the 2,2-azino-bis(3-ethylbenzothiazoline-6-sulfonic acid) and oxygen radical absorbance capacity assays.

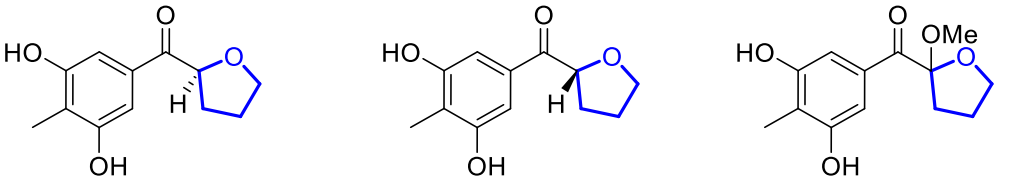

(-)-myrothecol **(-)-98** (+)-myrothecol **(+)-98** methoxy-myrothecol (**99**)

Figure 26. Structure of (-)-1*S*-myrothecol (**(-)-98**), (+)-1*R*-myrothecol (**(+)-98**), and methoxy-myrothecol(**99**).

4.1.3. Astrosphaeriella THFs

In 2016, astronypyrone (**100**), astronyquinone (**101**), and astronyurea(**102**) (Figure **27**) were isolated from the marine fungus *Astrosphaeriella nypae* BCC 5335 [91]. Compound **101** shows weak antituberculosis activity (with a MIC value of 50 μg/mL) and presents cytotoxicity against African green monkey kidney fibroblast cell lines (IC_{50}= 17.4 μg/mL).

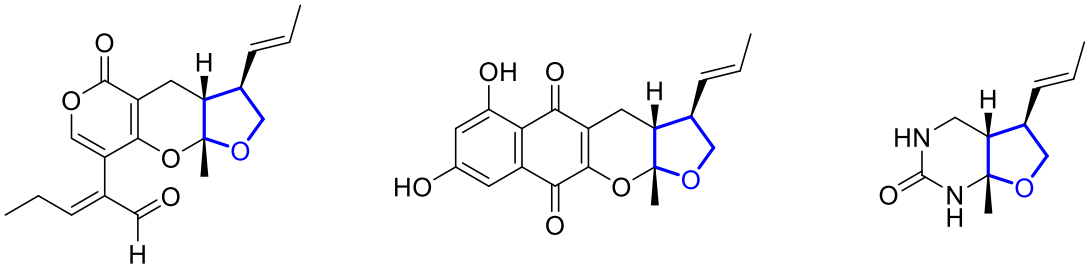

astronypyrone (**100**) astronyquinone (**101**) astronyurea (**102**)

Figure 27. Structure of astronypyrone (**100**), astronyquinone (**101**) and astronyurea (**102**).

4.1.4.Sinularones

Sinularones A-I were isolated in 2012 from the marine soft coral *Sinularia* sp. [92]. Their structures were elucidated by IR, MS, CD, 1D and 2D NMR. Among them, sinularones E (**103**) and F (**104**) contain a tetrahydrofuran moiety (**Figure 28**).

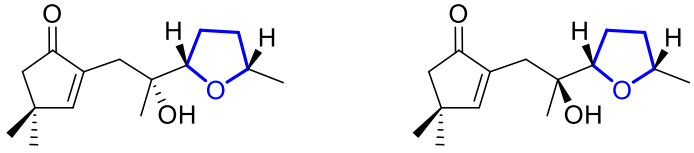

sinularone E (**103**) sinularone F (**104**)

Figure 28. Structure of sinularones E (**103**) and F (**104**).

Their first total synthesis, based on a hydrogenative metathesis of enynes, was reported in 2020 by Fürstner and coworkers [93]. The required 2,5-*cis*-tetrahydrofuran derivative **105** was readily obtained by hydrogenation (over Rh/Al_2O_3) of commercial furane **106**. Three further steps were needed to get silyl ether **107**, which in the presence

Preprints (www.preprints.org) | NOT PEER-REVIEWED | Posted: 21 September 2022 doi:10.20944/preprints202209.0320.v1

of ruthenium catalyst **108** and H_2 undergoes a hydrogenative metathesis. The later deprotection with TBAF, produces **103** with 65% yield over both steps. Sinularone F (**104**) synthesis utilizes the same strategy (Scheme **11**).

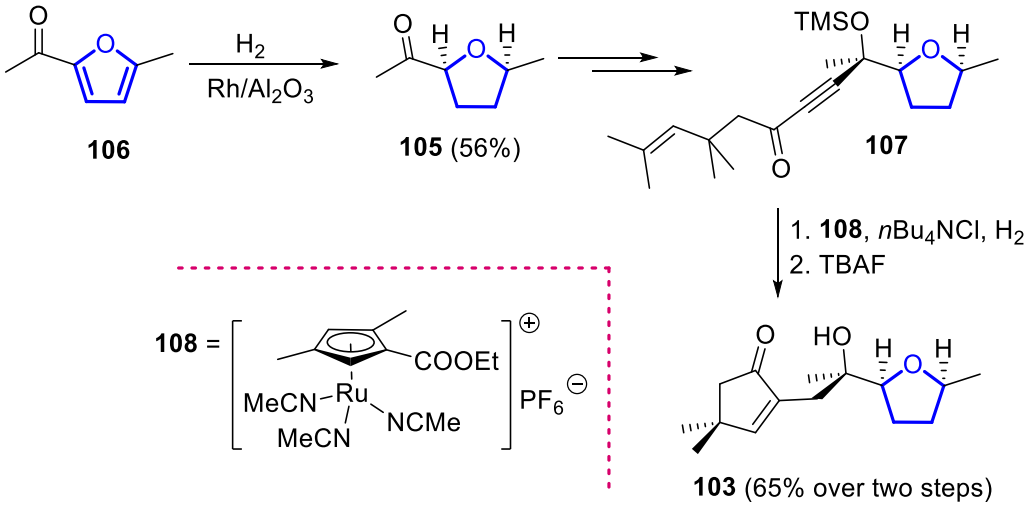

Scheme 11. Synthesis of sinularone E (**103**). A similar strategy was applied to sinularone F (**104**).

4.1.5. (+)-Varitriol

(+)-Varitriol (**(+)-109)** (Figure **29**) was isolated in 2002 from a marine-derived strain of the fungus *Emericella variecolor* [94]. Its structure and relative stereochemistry was determined by NMR studies. It displays low cytotoxic activity against leukemia, ovarian and colon cells, but its activity to renal, CNS and breast cancer cell lines was very promising (of the range of GI_{50} =1.63-2.44·10^{-7}M). In 2006, Jennings and coworkers achieved the first total synthesis of its enantiomer **(-)-109**, and thus determined its absolute stereochemistry [95].

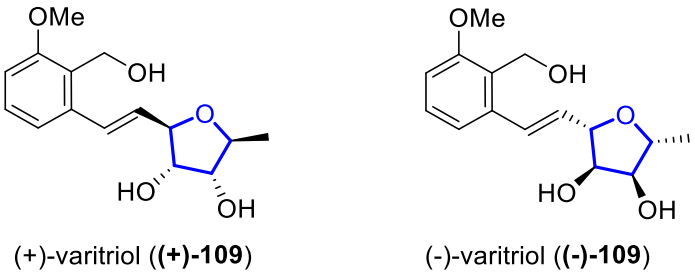

Figure 29. Structure of (+)-varitriol (**(+)-109**) and (-)-varitriol (**(-)-109**).

Its activity towards the mentioned cancer cell lines attracted the attention of synthetic chemists, an different synthetic approaches for **(+)-109** appeared in the next few years [96]. Taylor employed a known tetrahydrofuran-2,3,4-triol derivative as the starting material for the synthesis, in three further steps, of the desired**(-)-109** and its 3′-epi-derivative [97]. Srihari also achieved the synthesis of **(-)-109**, **(+)-109** and its 6′-epi-derivative starting from commercial D-(-)-ribose [98, 99]. Krause performed a modular synthesis of **(+)-109**, in 10 steps with an overall yield of 6,4% [100]. The key tetrahydrofuran with the appropriate four stereocenters **110** was prepared in four linear steps from a known enyne. Thus, Sharpless epoxidation and benzylation of (*E*)-hex-2-en-4-yn-1-ol provided propargyl epoxide **111** in 47% yield over two steps. A copper hydride-catalyzed reduction of **111**, followed by a gold-catalyzed cycloisomerization furnished the key dihydrofuranyl intermediate **112**, with two of the required stereogenic centers. Final Sharpless dihydroxylation of **112** afforded **110**, as a satisfactory 78:22 mixture of diastereoisomers. The desired natural product was obtained in four further steps.

Preprints (www.preprints.org) | NOT PEER-REVIEWED | Posted: 21 September 2022 doi:10.20944/preprints202209.0320.v1

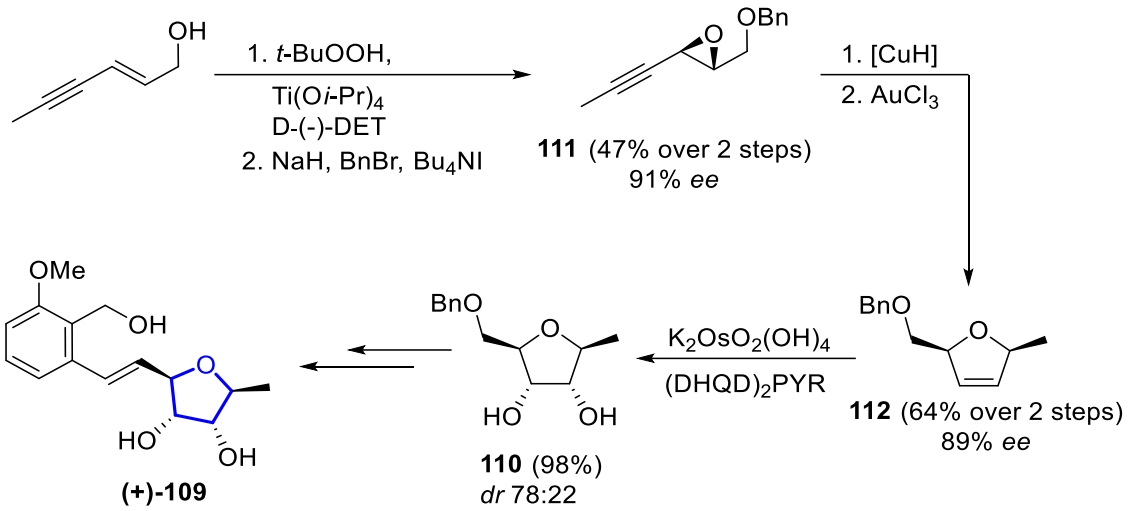

Scheme 12. Modular synthesis of (+)-varitriol (**(+)-109**) by Krause.

A recent example of the total synthesis of **(+)-109** was reported by Cordero-Vargas [101]. In this approach the tetrahydrofuranyl key intermediate **113**, bearing the four precise sterocenters, was obtained from commercial L-ribono-1,4-lactone in six steps. The key step in this process is the stereocontrolled nucleophilic addition to five-membered oxocarbenium ions directed by the protecting groups. Thus, TBS-protected lactone **114**, obtained in four conventional steps from L-ribono-1,4-lactone, undergoes acetylide addition an subsequent Lewis acid promoted oxocarbenium ion formation. The following stereoselective hydride attack provides tetrahydrofuran **113** as a single diastereomer in 60% yield. The final synthesis of **(+)-109** is achieved in four further steps with 31% yield over them (Scheme **13**).

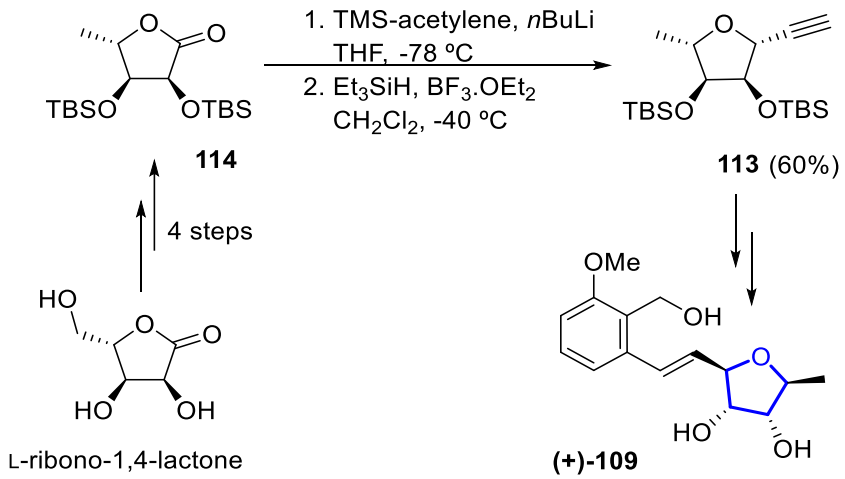

Scheme 13. Protecting group-directed nuclephilic addition for the synthesis of (+)-varitriol (**109**).

Later on, Qin developed a direct cross-coupling between terminal alkynes and glycosyl acetates, that was applied to the formal synthesiss of **(+)-109** and analogues [102]. More recently, Wang and coworkers reported another formal synthesis of **(+)-109** [103]. There, they developed a chromium-catalyzed enantioconvergent allenylation of aldehydes to synthesize α-allenols from racemic propargyl halides. Starting from silylated propargyl bromide **115** and benzyloxyacetaldehyde, allenol **116** can be accessed through the developed procedure. The chromium catalyst is formed in situ by the addition of chromium chloride, and the oxazoline ligand **(*R*,*S*)-117**. Manganese acts as reducing agent, and Cp_2ZrCl_2 as dissociation reagent. Then, removal of the silyl group with tetrabutylammonium fluoride gives advanced intermediate **118** in 82% yield, thus accomplishing the formal synthesis of the desired **(+)-109**.

Preprints (www.preprints.org) | NOT PEER-REVIEWED | Posted: 21 September 2022 doi:10.20944/preprints202209.0320.v1

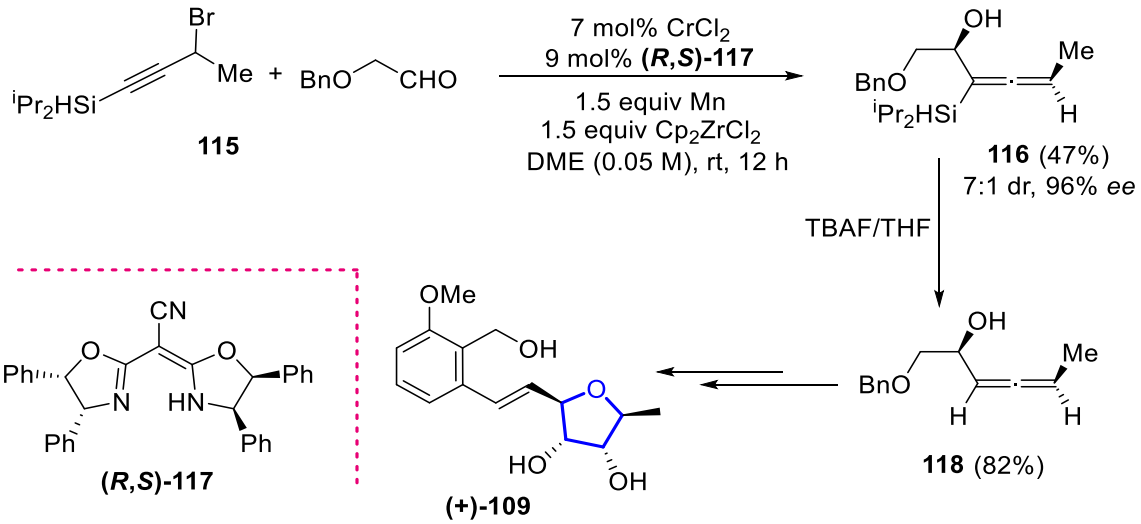

Scheme 14. Application of allenylation of aldehydes to the formal synthesis of (+)-varitriol by Wang.

5. Conclusions

Terpenes and related compounds represent an important family of marine-derived metabolites. The great number of studies focused on their biological activities and total synthesis remark their importance. Within heterocycles, the tetrahydrofuran moiety is a common motif found in a variety of such compounds, which has meant a particular emphasis of researchers on the development of new methodologies for the synthesis of such derivatives. In this context, total synthesis is a powerful tool to have access to these natural products. Firstly, it is an invaluable mean for the determination of the structure and total configuration of natural compounds, since in some cases the available NMR methods are insufficient to definitively determine the structures of biologically relevant substances. Secondly, since extracting and purifying compounds from natural sources is a difficult and time-consuming process, total synthesis has emerged as a suitable solution for the production of larger amounts of compounds, thus bringing possibilities of further biological studies, discovery of novel drug candidates and expansion of the medicinal chemistry frontiers.

Author Contributions: Writing—original draft preparation, L.F.-P. and P.G.-A.; writing—reviewing and editing, C.D.-P. and A.B. All authors have read and agreed to the published version of the manuscript.

Funding: This research was funded by "Junta de Castilla y León", grant number VA294-P18.

Acknowledgments: L. F.-P. and P. G.-A. acknowledge predoctoral Grants funded by the "Junta de Castilla y León" and the University of Valladolid, respectively.

Conflicts of Interest: "The authors declare no conflict of interest."

Abbreviations: BDSB: bromodiethylsulfonium bromopentachloroantimonate; Bn: benzyl; Boc: tert-butyloxy carbonyl; Bz: benzoyl; CSA camphorsulfonic acid; Cy: cyclohexyl; D-(-)-DET: (-)-diethyl D-tartrate; $(DHQD)_2PYR$: hydroquinidine-2,5-diphenyl-4,6-pyrimidinediyl diether; DME: dimethoxyethane; DMSO: dimethylsulfoxide; IBX: orto-iodoxybenzoic acid; Ms: methanesulfonyl; TBAF: tetrabutylammonium fluoride; TBHP: tert-butyl hydroperoxide; TfOH: trifluoromethanesulfonic acid; TMS: trimethylsilyl.

References

1. Fuwa, H. Structure determination, correction, and disproof of marine macrolide natural products by chemical synthesis. *Org. Chem. Front.* **2021**, *8*, 3990-4023, https://doi.org/10.1039/D1QO00481F.
2. Ebel, R. Terpenes from Marine-Derived Fungi. *Mar. Drugs* **2010**, *8*, 2340-2368, https://doi.org/10.3390/md8082340.

3. Elissawy, A. M.; El-Shazly, M.; Ebada, S. S.; Singab, A. B.; Proksch, P. Bioactive Terpenes from Marine-Derived Fungi. *Mar. Drugs* **2015**, *13*, 1966-1992, https://doi.org/10.3390/md13041966.
4. Jiang, M.; Wu, Z.; Guo, H.; Liu, L.; Chen, S. A Review of Terpenes from Marine-Derived Fungi: 2015–2019. *Mar. Drugs* **2020**, *18*, 321, https://doi.org/10.3390/md18060321.
5. Nasir, N. M.; Ermanis, K.; Clarke, P. A. Strategies for the construction of tetrahydropyran rings in the synthesis of natural products. *Org. Biomol. Chem.* **2014**, *12*, 3323-3335, https://doi.org/10.1039/C4OB00423J.
6. Fuwa, H. Contemporary Strategies for the Synthesis of Tetrahydropyran Derivatives: Application to Total Synthesis of Neopeltolide, a Marine Macrolide Natural Product. *Mar. Drugs* **2016**, *14*, 65, https://doi.org/doi:10.3390/md14040065.
7. Barbero, H.; Díez-Poza, C.; Barbero, A. The Oxepane Motif in Marine Drugs. *Marine Drugs* **2017**, *15*, https://doi.org/10.3390/md15110361.
8. Fernandes, R. A.; Pathare, R. S.; Gorve, D. A. Advances in Total Synthesis of Some 2,3,5-Trisubstituted Tetrahydrofuran Natural Products. *Chemistry – An Asian Journal* **2020**, *15*, 2815-2837, https://doi.org/10.1002/asia.202000753.
9. Fernandes, R. A.; Gorve, D. A.; Pathare, R. S. Emergence of 2,3,5-trisubstituted tetrahydrofuran natural products and their synthesis. *Org. Biomol. Chem.* **2020**, *18*, 7002-7025, https://doi.org/10.1039/D0OB01542C.
10. Fernández-Peña, L.; Díez-Poza, C.; González-Andrés, P.; Barbero, A. The Tetrahydrofuran Motif in Polyketide Marine Drugs. *Mar. Drugs* **2022**, *20*, 120, https://doi.org/10.3390/md20020120.
11. Warren, R. G.; Wells, R. J.; Blount, J. F. A novel lipid from the brown alga Notheia anomala. *Aust. J. Chem.* **1980**, *33*, 891-898, https://doi.org/10.1071/CH9800891.
12. Capon, R. J.; A Barrow, R.; Rochfort, S.; Jobling, M.; Skene, C.; Lacey, E.; H Gill, J.; Friedel, T.; Wadsworth, D. Marine nematocides: Tetrahydrofurans from a southern Australian brown alga, Notheia anomala. *Tetrahedron* **1998**, *54*, 2227-2242, https://doi.org/10.1016/S0040-4020(97)10432-X.
13. Fernandes, R. A.; Pathare, R. S.; Gorve, D. A. Advances in Total Synthesis of Some 2,3,5-Trisubstituted Tetrahydrofuran Natural Products. *Chem. Asian J.* **2020**, *15*, 2815-2837, https://doi.org/10.1002/asia.202000753.
14. Li, K.; Huertas, M.; Brant, C.; Chung-Davidson, Y.-W.; Bussy, U.; Hoye, T. R.; Li, W. (+)- and (−)-Petromyroxols: Antipodal Tetrahydrofurandiols from Larval Sea Lamprey (Petromyzon marinus L.) That Elicit Enantioselective Olfactory Responses. *Org. Lett.* **2015**, *17*, 286-289, https://doi.org/10.1021/ol5033893.
15. Mullapudi, V.; Ahmad, I.; Senapati, S.; Ramana, C. V. Total Synthesis of (+)-Petromyroxol, (−)-iso-Petromyroxol, and Possible Diastereomers. *ACS Omega* **2020**, *5*, 25334-25348, https://doi.org/10.1021/acsomega.0c03674.
16. Li, K.; Brant, C. O.; Huertas, M.; Hessler, E. J.; Mezei, G.; Scott, A. M.; Hoye, T. R.; Li, W. Fatty-acid derivative acts as a sea lamprey migratory pheromone. *PNAS* **2018**, *115*, 8603, https://doi.org/10.1073/pnas.1803169115.
17. Morinaka, B. I.; Skepper, C. K.; Molinski, T. F. Ene-yne Tetrahydrofurans from the Sponge Xestospongia muta. Exploiting a Weak CD Effect for Assignment of Configuration. *Org. Lett.* **2007**, *9*, 1975-1978, https://doi.org/10.1021/ol0705696.
18. Zhou, X.; Lu, Y.; Lin, X.; Yang, B.; Yang, X.; Liu, Y. Brominated aliphatic hydrocarbons and sterols from the sponge Xestospongia testudinaria with their bioactivities. *Chem. Phys. Lipids* **2011**, *164*, 703-706, https://doi.org/10.1016/j.chemphyslip.2011.08.002.
19. Liu, Y.; Ding, L.; Zhang, Z.; Yan, X.; He, S. New antifungal tetrahydrofuran derivatives from a marine sponge-associated fungus Aspergillus sp. LS78. *Fitoterapia* **2020**, *146*, 104677, https://doi.org/10.1016/j.fitote.2020.104677.
20. Cueto, M.; Darias, J. Uncommon tetrahydrofuran monoterpenes from Antarctic Pantoneura plocamioides. *Tetrahedron* **1996**, *52*, 5899-5906, https://doi.org/10.1016/0040-4020(96)00220-7.
21. Blanc, A.; Toste, F. D. Enantioselective Synthesis of Cyclic Ethers through a Vanadium-Catalyzed Resolution/Oxidative Cyclization. *Angew. Chem. Int. Ed.* **2006**, *45*, 2096-2099, https://doi.org/10.1002/anie.200503852.
22. Darias, J.; Rovirosa, J.; San Martin, A.; Díaz, A.-R.; Dorta, E.; Cueto, M. Furoplocamioids A− C, Novel Polyhalogenated Furanoid Monoterpenes from Plocamium c artilagineum. *J. Nat. Prod.* **2001**, *64*, 1383-1387, https://doi.org/10.1021/np010297u.

23. Díaz-Marrero, A. R.; Cueto, M.; Dorta, E.; Rovirosa, J.; San-Martín, A.; Darias, J. New halogenated monoterpenes from the red alga Plocamium cartilagineum. *Tetrahedron* **2002**, *58*, 8539-8542, https://doi.org/10.1016/S0040-4020(02)01019-0.
24. Argandoña, V. H.; Rovirosa, J.; San-Martín, A.; Riquelme, A.; Díaz-Marrero, A. R.; Cueto, M.; Darias, J.; Santana, O.; Guadaño, A.; González-Coloma, A. Antifeedant Effects of Marine Halogenated Monoterpenes. *J. Agric. Food. Chem.* **2002**, *50*, 7029-7033, https://doi.org/10.1021/jf025857p.
25. Raju, R.; Piggott, A. M.; Barrientos Diaz, L. X.; Khalil, Z.; Capon, R. J. Heronapyrroles A−C: Farnesylated 2-Nitropyrroles from an Australian Marine-Derived Streptomyces sp. *Org. Lett.* **2010**, *12*, 5158-5161, https://doi.org/10.1021/ol102162d.
26. Schmidt, J.; Khalil, Z.; Capon, R. J.; Stark, C. B. Heronapyrrole D: A case of co-inspiration of natural product biosynthesis, total synthesis and biodiscovery. *Beilstein J. Org. Chem.* **2014**, *10*, 1228-1232, https://doi.org/10.3762/bjoc.10.121.
27. Schmidt, J.; Stark, C. B. W. Biomimetic Synthesis and Proposal of Relative and Absolute Stereochemistry of Heronapyrrole C. *Org. Lett.* **2012**, *14*, 4042-4045, https://doi.org/10.1021/ol300954s.
28. Schmidt, J.; Stark, C. B. W. Synthetic Endeavors toward 2-Nitro-4-Alkylpyrroles in the Context of the Total Synthesis of Heronapyrrole C and Preparation of a Carboxylate Natural Product Analogue. *J. Org. Chem.* **2014**, *79*, 1920-1928, https://doi.org/10.1021/jo402240g.
29. Ding, X.-B.; Furkert, D. P.; Capon, R. J.; Brimble, M. A. Total Synthesis of Heronapyrrole C. *Org. Lett.* **2014**, *16*, 378-381, https://doi.org/10.1021/ol403246j.
30. Ding, X.-B.; Brimble, M. A.; Furkert, D. P. Nitropyrrole natural products: isolation, biosynthesis and total synthesis. *Org. Biomol. Chem.* **2016**, *14*, 5390-5401, https://doi.org/10.1039/C5OB02599K.
31. Ding, X.-B.; Furkert, D. P.; Brimble, M. A. 2-Nitropyrrole cross-coupling enables a second generation synthesis of the heronapyrrole antibiotic natural product family. *Chem. Commun.* **2016**, *52*, 12638-12641, https://doi.org/10.1039/C6CC07532K.
32. Ding, X.-B.; Brimble, M. A.; Furkert, D. P. Reactivity of 2-Nitropyrrole Systems: Development of Improved Synthetic Approaches to Nitropyrrole Natural Products. *J. Org. Chem.* **2018**, *83*, 12460-12470, https://doi.org/10.1021/acs.joc.8b01692.
33. Suzuki, T.; Koizumi, K.; Suzuki, M.; Kurosawa, E. Kumausalle, a new bromoallene from the marine red alga laurencia nipponica yamada *Chem. Lett.* **1983**, *12*, 1639-1642, https://doi.org/10.1246/cl.1983.1639.
34. Grese, T. A.; Hutchinson, K. D.; Overman, L. E. General approach to halogenated tetrahydrofuran natural products from red algae of the genus Laurencia. Total synthesis of (.+-.)-kumausallene and (.+-.)-1-epi-kumausallene. *J. Org. Chem.* **1993**, *58*, 2468-2477, https://doi.org/10.1021/jo00061a021.
35. Werness, J. B.; Tang, W. Stereoselective Total Synthesis of (−)-Kumausallene. *Org. Lett.* **2011**, *13*, 3664-3666, https://doi.org/10.1021/ol201477u.
36. Das, S.; Ramana, C. V. A formal total synthesis of (−)-kumausallene. *Tetrahedron* **2015**, *71*, 8577-8584, https://doi.org/10.1016/j.tet.2015.09.027.
37. Suzuki, T.; Koizumi, K.; Suzuki, M.; Kurosawa, E. Kumausynes and deacetylkumausynes, four new halogenated C-15 acetylenes from the red alga Laurencia nipponica Yamada. *Chem. Lett.* **1983**, *12*, 1643-1644, https://doi.org/10.1246/cl.1983.1643.
38. Brown, M. J.; Harrison, T.; Overman, L. E. General approach to halogenated tetrahydrofuran natural products from red algae of the genus Laurencia. Total synthesis of (.+-.)-trans-kumausyne and demonstration of an asymmetric synthesis strategy. *J. Am. Chem. Soc.* **1991**, *113*, 5378-5384, https://doi.org/10.1021/ja00014a032.
39. von Salm, J. L.; Witowski, C. G.; Fleeman, R. M.; McClintock, J. B.; Amsler, C. D.; Shaw, L. N.; Baker, B. J. Darwinolide, a New Diterpene Scaffold That Inhibits Methicillin-Resistant Staphylococcus aureus Biofilm from the Antarctic Sponge Dendrilla membranosa. *Org. Lett.* **2016**, *18*, 2596-2599, https://doi.org/10.1021/acs.orglett.6b00979.
40. Shilling, A. J.; Witowski, C. G.; Maschek, J. A.; Azhari, A.; Vesely, B. A.; Kyle, D. E.; Amsler, C. D.; McClintock, J. B.; Baker, B. J. Spongian Diterpenoids Derived from the Antarctic Sponge Dendrilla antarctica Are Potent Inhibitors of the Leishmania Parasite. *J. Nat. Prod.* **2020**, *83*, 1553-1562, https://doi.org/10.1021/acs.jnatprod.0c00025.

41. Siemon, T.; Steinhauer, S.; Christmann, M. Synthesis of (+)-Darwinolide, a Biofilm-Penetrating Anti-MRSA Agent. *Angew. Chem. Int. Ed.* **2019**, *58*, 1120-1122, https://doi.org/10.1002/anie.201813142.
42. Rodríguez, A. D.; Piña, I. C.; Soto, J. J.; Rojas, D. R.; Barnes, C. L. Isolation and structures of the uprolides. I. Thirteen new cytotoxic cembranolides from the Caribbean gorgonian Euniceamammosa. *Can. J. Chem.* **1995**, *73*, 643-654, https://doi.org/10.1139/v95-083.
43. Rodríguez, A. D.; Soto, J. J.; Piña, I. C. Uprolides D-G, 2. A Rare Family of 4,7-Oxa-bridged Cembranolides from the Caribbean Gorgonian Eunicea mammosa. *J. Nat. Prod.* **1995**, *58*, 1209-1216, https://doi.org/10.1021/np50122a008.
44. Rodríguez, A. D.; Soto, J. J.; Barnes, C. L. Synthesis of Uprolide D− G Analogues. Revision of Structure of the Marine Cembranolides Uprolide F Diacetate and Uprolide G Acetate. *J. Org. Chem.* **2000**, *65*, 7700-7702, https://doi.org/10.1021/jo000996w.
45. Zhu, L.; Tong, R. Structural Revision of (+)-Uprolide F Diacetate Confirmed by Asymmetric Total Synthesis. *Org. Lett.* **2015**, *17*, 1966-1969, https://doi.org/10.1021/acs.orglett.5b00700.
46. Zhu, L.; Liu, Y.; Ma, R.; Tong, R. Total Synthesis and Structural Revision of (+)-Uprolide G Acetate. *Angew. Chem. Int. Ed.* **2015**, *54*, 627-632, https://doi.org/10.1002/anie.201409618.
47. Zhu, L.; Tong, R. Structural Revision of Uprolide G Acetate: Effective Interplay between NMR Data Analysis and Chemical Synthesis. *Synlett* **2015**, *26*, 1643-1648, https://doi.org/10.1055/s-0034-1380616.
48. Ramana, C. V.; Salian, S. R.; Gurjar, M. K. Central core of uprolides D and E: a survey of some ring closing metathesis approaches. *Tetrahedron Lett.* **2007**, *48*, 1013-1016, https://doi.org/10.1016/j.tetlet.2006.11.176.
49. Marshall, J. A.; Griot, C. A.; Chobanian, H. R.; Myers, W. H. Synthesis of a Lactone Diastereomer of the Cembranolide Uprolide D. *Org. Lett.* **2010**, *12*, 4328-4331, https://doi.org/10.1021/ol101776e.
50. Torres-Mendoza, D.; González, Y.; Gómez-Reyes, J. F.; Guzmán, H. M.; López-Perez, J. L.; Gerwick, W. H.; Fernandez, P. L.; Gutiérrez, M. Uprolides N, O and P from the Panamanian Octocoral Eunicea succinea. *Molecules* **2016**, *21*, https://doi.org/10.3390/molecules21060819.
51. Suzuki, M.; Matsuo, Y.; Takeda, S.; Suzuki, T. Intricatetraol, a halogenated triterpene alcohol from the red alga Laurencia intricata. *Phytochemistry* **1993**, *33*, 651-656, https://doi.org/10.1016/0031-9422(93)85467-6.
52. Morimoto, Y.; Takaishi, M.; Adachi, N.; Okita, T.; Yata, H. Two-directional synthesis and stereochemical assignment toward a C2 symmetric oxasqualenoid (+)-intricatetraol. *Org. Biomol. Chem.* **2006**, *4*, 3220-3222, https://doi.org/10.1039/B608098G.
53. Morimoto, Y.; Okita, T.; Takaishi, M.; Tanaka, T. Total Synthesis and Determination of the Absolute Configuration of (+)-Intricatetraol. *Angew. Chem. Int. Ed.* **2007**, *46*, 1132-1135, https://doi.org/10.1002/anie.200603806.
54. Matsuo, Y.; Suzuki, M.; Masuda, M.; Iwai, T.; Morimoto, Y. Squalene-Derived Triterpene Polyethers from the Red Alga Laurencia omaezakiana. *Helv. Chim. Acta* **2008**, *91*, 1261-1266, https://doi.org/10.1002/hlca.200890137.
55. Morimoto, Y.; Okita, T.; Kambara, H. Total Synthesis and Determination of the Absolute Configuration of (+)-Omaezakianol. *Angew. Chem. Int. Ed.* **2009**, *48*, 2538-2541, https://doi.org/10.1002/anie.200805857.
56. Xiong, Z.; Busch, R.; Corey, E. J. A Short Total Synthesis of (+)-Omaezakianol via an Epoxide-Initiated Cationic Cascade Reaction. *Org. Lett.* **2010**, *12*, 1512-1514, https://doi.org/10.1021/ol100213e.
57. Morimoto, Y.; Takeuchi, E.; Kambara, H.; Kodama, T.; Tachi, Y.; Nishikawa, K. Biomimetic Epoxide-Opening Cascades of Oxasqualenoids Triggered by Hydrolysis of the Terminal Epoxide. *Org. Lett.* **2013**, *15*, 2966-2969, https://doi.org/10.1021/ol401081e.
58. Itokawa, H.; Kishi, E.; Morita, H.; Takeya, K.; Iitaka, Y. A New Squalene-type Triterpene from the Woods of Eurycoma longifolia. *Chem. Lett.* **1991**, *20*, 2221-2222, https://doi.org/10.1246/cl.1991.2221.
59. Morita, H.; Kishi, E.; Takeya, K.; Itokawa, H.; Iitaka, Y. Squalene derivatives from Eurycoma longifolia. *Phytochemistry* **1993**, *34*, 765-771, https://doi.org/10.1016/0031-9422(93)85356-V.

60. Morimoto, Y.; Iwai, T.; Kinoshita, T. Total synthesis and determination of the absolute configuration of (−)-longilene peroxide. *Tetrahedron Lett.* **2001**, *42*, 6307-6309, https://doi.org/10.1016/S0040-4039(01)01239-4.
61. Morimoto, Y.; Iwai, T.; Nishikawa, Y.; Kinoshita, T. Stereospecific and biomimetic synthesis of CS and C2 symmetric 2,5-disubstituted tetrahydrofuran rings as central building blocks of biogenetically intriguing oxasqualenoids. *Tetrahedron: Asymmetry* **2002**, *13*, 2641-2647, https://doi.org/10.1016/S0957-4166(02)00718-8.
62. Cen-Pacheco, F.; Pérez Manríquez, C.; Luisa Souto, M.; Norte, M.; Fernández, J. J.; Hernández Daranas, A. Marine Longilenes, Oxasqualenoids with Ser-Thr Protein Phosphatase 2A Inhibition Activity. *Mar. Drugs* **2018**, *16*, https://doi.org/10.3390/md16040131.
63. Cen-Pacheco, F.; Santiago-Benítez, A. J.; Tsui, K. Y.; Tantillo, D. J.; Fernández, J. J.; Daranas, A. H. Structure and Computational Basis for Backbone Rearrangement in Marine Oxasqualenoids. *J. Org. Chem.* **2021**, *86*, 2437-2446, https://doi.org/10.1021/acs.joc.0c02600.
64. Norte, M.; Fernández, J.; Souto, M. L.; Gavín, J.; García-Grávalos, M. D. Thyrsenols A and B, two unusual polyether squalene derivatives. *Tetrahedron* **1997**, *53*, 3173-3178, https://doi.org/10.1016/S0040-4020(97)00028-8.
65. Fernández, J.; Souto, M. L.; Norte, M. Evaluation of the cytotoxic activity of polyethers isolated from Laurencia. *Biorg. Med. Chem.* **1998**, *6*, 2237-2243, https://doi.org/10.1016/S0968-0896(98)80004-7.
66. Souto, M. a. L.; Manríquez, C. P.; Norte, M.; Leira, F.; Fernández, J. J. The inhibitory effects of squalene-derived triterpenes on protein phosphatase PP2A. *Bioorg. Med. Chem. Lett.* **2003**, *13*, 1261-1264, https://doi.org/10.1016/S0960-894X(03)00136-7.
67. Cen-Pacheco, F.; Villa-Pulgarin, J. A.; Mollinedo, F.; Norte, M.; Daranas, A. H.; Fernández, J. J. Cytotoxic oxasqualenoids from the red alga Laurencia viridis. *Eur. J. Med. Chem.* **2011**, *46*, 3302-3308, https://doi.org/10.1016/j.ejmech.2011.04.051.
68. Cen-Pacheco, F.; Mollinedo, F.; Villa-Pulgarín, J. A.; Norte, M.; Fernández, J. J.; Hernández Daranas, A. Saiyacenols A and B: the key to solve the controversy about the configuration of aplysiols. *Tetrahedron* **2012**, *68*, 7275-7279, https://doi.org/10.1016/j.tet.2012.07.005.
69. Cen-Pacheco, F.; Santiago-Benítez, A. J.; García, C.; Álvarez-Méndez, S. J.; Martín-Rodríguez, A. J.; Norte, M.; Martín, V. S.; Gavín, J. A.; Fernández, J. J.; Daranas, A. H. Oxasqualenoids from Laurencia viridis: Combined Spectroscopic–Computational Analysis and Antifouling Potential. *J. Nat. Prod.* **2015**, *78*, 712-721, https://doi.org/10.1021/np5008922.
70. Díaz-Marrero, A. R.; López-Arencibia, A.; Bethencout-Estrella, C. J.; Cen-Pacheco, F.; Sifaoui, I.; Hernández Creus, A.; Duque-Ramírez, M. C.; Souto, M. L.; Hernández Daranas, A.; Lorenzo-Morales, J.; Piñero, J. E.; Fernández, J. J. Antiprotozoal activities of marine polyether triterpenoids. *Bioorg. Chem.* **2019**, *92*, 103276, https://doi.org/10.1016/j.bioorg.2019.103276.
71. Nishikibe, K.; Nishikawa, K.; Kumagai, M.; Doe, M.; Morimoto, Y. Asymmetric Total Syntheses, Stereostructures, and Cytotoxicities of Marine Bromotriterpenoids Aplysiol B (Laurenmariannol) and Saiyacenol A. *Chem. Asian J.* **2022**, *17*, e202101137, https://doi.org/10.1002/asia.202101137.
72. Suzuki, T.; Suzuki, M.; Furusaki, A.; Matsumoto, T.; Kato, A.; Imanaka, Y.; Kurosawa, E. Teurilene and thyrsiferyl 23-acetate, meso and remarkably cytotoxic compounds from the marine red alga laurencia obtusa (hudson) lamouroux. *Tetrahedron Lett.* **1985**, *26*, 1329-1332, https://doi.org/10.1016/S0040-4039(00)94885-8.
73. Sheikh, N. S. Synthetic endeavours towards oxasqualenoid natural products containing 2,5-disubstituted tetrahydrofurans – eurylene and teurilene. *Nat. Prod. Rep.* **2014**, *31*, 1088-1100, https://doi.org/10.1039/C4NP00029C.
74. Blunt, J. W.; Hartshorn, M. P.; McLennan, T. J.; Munro, M. H. G.; Robinson, W. T.; Yorke, S. C. Thyrsiferol: a squalene-derived metabolite of laurencia thyrsifera. *Tetrahedron Lett.* **1978**, *19*, 69-72, https://doi.org/10.1016/S0040-4039(01)88986-3.
75. Sakemi, S.; Higa, T.; Jefford, C. W.; Bernardinelli, G. Venustatriol. A new, anti-viral, triterpene tetracyclic ether from Laurencia venusta. *Tetrahedron Lett.* **1986**, *27*, 4287-4290, https://doi.org/10.1016/S0040-4039(00)94254-0.

76. Little, R. D.; Nishiguchi, G. A., Synthetic Efforts Toward, and Biological Activity of, Thyrsiferol and Structurally-Related Analogues. In *Stud. Nat. Prod. Chem.*, Atta ur, R., Ed. Elsevier: 2008; Vol. 35, pp 3-56.
77. Lorenzo-Morales, J.; Díaz-Marrero, A. R.; Cen-Pacheco, F.; Sifaoui, I.; Reyes-Batlle, M.; Souto, M. L.; Hernández Daranas, A.; Piñero, J. E.; Fernández, J. J. Evaluation of Oxasqualenoids from the Red Alga Laurencia viridis against Acanthamoeba. *Mar. Drugs* **2019**, *17*, https://doi.org/10.3390/md17070420.
78. Hirashima, M.; Tsuda, K.; Hamada, T.; Okamura, H.; Furukawa, T.; Akiyama, S.-i.; Tajitsu, Y.; Ikeda, R.; Komatsu, M.; Doe, M.; Morimoto, Y.; Shiro, M.; van Soest, R. W. M.; Takemura, K.; Iwagawa, T. Cytotoxic Isomalabaricane Derivatives and a Monocyclic Triterpene Glycoside from the Sponge Rhabdastrella globostellata. *J. Nat. Prod.* **2010**, *73*, 1512-1518, https://doi.org/10.1021/np100302a.
79. Lai, K.-H.; Huang, Z.-H.; El-Shazly, M.; Peng, B.-R.; Wei, W.-C.; Su, J.-H. Isomalabaricane Triterpenes from the Marine Sponge Rhabdastrella sp. *Mar. Drugs* **2021**, *19*, https://doi.org/10.3390/md19040206.
80. Desoubzdanne, D.; Marcourt, L.; Raux, R.; Chevalley, S.; Dorin, D.; Doerig, C.; Valentin, A.; Ausseil, F.; Debitus, C. Alisiaquinones and alisiaquinol, dual inhibitors of Plasmodium falciparum enzyme targets from a New Caledonian deep water sponge. *J. Nat. Prod.* **2008**, *71*, 1189-1192, https://doi.org/10.1021/np8000909.
81. Shi, Z.-Z.; Miao, F.-P.; Fang, S.-T.; Liu, X.-H.; Yin, X.-L.; Ji, N.-Y. Sesteralterin and Tricycloalterfurenes A-D: Terpenes with Rarely Occurring Frameworks from the Marine-Alga-Epiphytic Fungus Alternaria alternata k21-1. *J. Nat. Prod.* **2017**, *80*, 2524-2529, https://doi.org/10.1021/acs.jnatprod.7b00478.
82. Hwang, J.-Y.; Park, S. C.; Byun, W. S.; Oh, D.-C.; Lee, S. K.; Oh, K.-B.; Shin, J. Bioactive Bianthraquinones and Meroterpenoids from a Marine-Derived Stemphylium sp. Fungus. *Mar. Drugs* **2020**, *18*, https://doi.org/10.3390/md18090436.
83. Fraga, B. M.; Díaz, C. E. Proposal for structural revision of several monosubstituted tricycloalternarenes. *Phytochemistry* **2022**, *198*, 113141, https://doi.org/10.1016/j.phytochem.2022.113141.
84. Duan, X.; Tan, X.; Gu, L.; Liu, J.; Hao, X.; Tao, L.; Feng, H.; Cao, Y.; Shi, Z.; Duan, Y.; Deng, M.; Chen, G.; Qi, C.; Zhang, Y. New secondary metabolites with immunosuppressive activity from the phytopathogenic fungus Bipolaris maydis. *Bioorg. Chem.* **2020**, *99*, 103816, https://doi.org/10.1016/j.bioorg.2020.103816.
85. Shi, X.; Wei, W.; Zhang, W.-J.; Hua, C.-P.; Chen, C.-J.; Ge, H.-M.; Tan, R.-X.; Jiao, R.-H. New tricycloalternarenes from fungus Alternaria sp. *J. Asian Nat. Prod. Res.* **2015**, *17*, 143-148, https://doi.org/10.1080/10286020.2014.970536.
86. Kim, M. C.; Winter, J. M.; Asolkar, R. N.; Boonlarppradab, C.; Cullum, R.; Fenical, W. Marinoterpins A–C: Rare Linear Merosesterterpenoids from Marine-Derived Actinomycete Bacteria of the Family Streptomycetaceae. *J. Org. Chem.* **2021**, *86*, 11140-11148, https://doi.org/10.1021/acs.joc.1c00262.
87. Kuroda, I.; Musman, M.; Ohtani, I. I.; Ichiba, T.; Tanaka, J.; Gravalos, D. G.; Higa, T. Pachastrissamine, a Cytotoxic Anhydrophytosphingosine from a Marine Sponge, Pachastrissa sp. *J. Nat. Prod.* **2002**, *65*, 1505-1506, https://doi.org/10.1021/np010659y.
88. Ledroit, V.; Debitus, C.; Lavaud, C.; Massiot, G. Jaspines A and B: two new cytotoxic sphingosine derivatives from the marine sponge Jaspis sp. *Tetrahedron Lett.* **2003**, *44*, 225-228, https://doi.org/10.1016/S0040-4039(02)02541-8.
89. Martinková, M.; Gonda, J. Marine cytotoxic jaspine B and its stereoisomers: biological activity and syntheses. *Carbohydr. Res.* **2016**, *423*, 1-42, https://doi.org/10.1016/j.carres.2016.01.009.
90. Lu, X.; He, J.; Wu, Y.; Du, N.; Li, X.; Ju, J.; Hu, Z.; Umezawa, K.; Wang, L. Isolation and Characterization of New Anti-Inflammatory and Antioxidant Components from Deep Marine-Derived Fungus Myrothecium sp. Bzo-l062. *Mar. Drugs* **2020**, *18*, https://doi.org/10.3390/md18120597.
91. Chokpaiboon, S.; Unagul, P.; Kongthong, S.; Danwisetkanjana, K.; Pilantanapak, A.; Suetrong, S.; Bunyapaiboonsri, T. A pyrone, naphthoquinone, and cyclic urea from the marine-derived fungus Astrosphaeriella nypae BCC 5335. *Tetrahedron Lett.* **2016**, *57*, 1171-1173, https://doi.org/10.1016/j.tetlet.2016.02.002.

92. Shi, H.; Yu, S.; Liu, D.; Van Ofwegen, L.; Proksch, P.; Lin, W. Sinularones A–I, New Cyclopentenone and Butenolide Derivatives from a Marine Soft Coral Sinularia sp. and Their Antifouling Activity. *Mar. Drugs* **2012**, *10*, https://doi.org/10.3390/md10061331.
93. Peil, S.; Bistoni, G.; Goddard, R.; Fürstner, A. Hydrogenative Metathesis of Enynes via Piano-Stool Ruthenium Carbene Complexes Formed by Alkyne gem-Hydrogenation. *J. Am. Chem. Soc.* **2020**, *142*, 18541-18553, https://doi.org/10.1021/jacs.0c07808.
94. Malmstrøm, J.; Christophersen, C.; Barrero, A. F.; Oltra, J. E.; Justicia, J.; Rosales, A. Bioactive Metabolites from a Marine-Derived Strain of the Fungus Emericella variecolor. *J. Nat. Prod.* **2002**, *65*, 364-367, https://doi.org/10.1021/np0103214.
95. Clemens, R. T.; Jennings, M. P. An efficient total synthesis and absolute configuration determination of varitriol. *Chem. Commun.* **2006**, 2720-2721, https://doi.org/10.1039/b603931f.
96. Mahesh, S. M.; Supriya, T.; Prakash, T. P. Recent Developments Towards the Synthesis of Varitriol: An Antitumour Agent from Marine Derived Fungus Emericella Variecolor. *Curr. Org. Synth.* **2014**, *11*, 268-287, https://doi.org/10.2174/15701794106661311241342 00.
97. McAllister, G. D.; Robinson, J. E.; Taylor, R. J. K. The synthesis of (−)-varitriol and (−)-3′-epi-varitriol via a Ramberg–Bäcklund route. *Tetrahedron* **2007**, *63*, 12123-12130, https://doi.org/10.1016/j.tet.2007.09.057.
98. Vamshikrishna, K.; Srihari, P. A conventional approach to the total synthesis of (−)-varitriol. *Tetrahedron: Asymmetry* **2012**, *23*, 1584-1587, https://doi.org/10.1016/j.tetasy.2012.10.010.
99. Vamshikrishna, K.; Srihari, P. Total synthesis of (+)-varitriol and (+)-6′-epi-varitriol. *Tetrahedron* **2012**, *68*, 1540-1546, https://doi.org/10.1016/j.tet.2011.12.008.
100. Sun, T.; Deutsch, C.; Krause, N. Combined coinage metal catalysis in natural product synthesis: total synthesis of (+)-varitriol and seven analogs. *Org. Biomol. Chem.* **2012**, *10*, 5965-5970, https://doi.org/10.1039/C2OB25069A.
101. Sánchez-Eleuterio, A.; García-Santos, W. H.; Díaz-Salazar, H.; Hernández-Rodríguez, M.; Cordero-Vargas, A. Stereocontrolled Nucleophilic Addition to Five-Membered Oxocarbenium Ions Directed by the Protecting Groups. Application to the Total Synthesis of (+)-Varitriol and of Two Diastereoisomers Thereof. *J. Org. Chem.* **2017**, *82*, 8464-8475, https://doi.org/10.1021/acs.joc.7b01211.
102. He, H.; Qin, H.-B. ZnBr2-catalyzed direct C-glycosylation of glycosyl acetates with terminal alkynes. *Org. Chem. Front.* **2018**, *5*, 1962-1966, https://doi.org/10.1039/C8QO00380G.
103. Zhang, F.-H.; Guo, X.; Zeng, X.; Wang, Z. Catalytic Enantioconvergent Allenylation of Aldehydes with Propargyl Halides. *Angew. Chem. Int. Ed.* **2022**, *61*, e202117114, https://doi.org/10.1002/anie.202117114.